

This article was downloaded by:

On: 21 January 2011

Access details: *Access Details: Free Access*

Publisher *Taylor & Francis*

Informa Ltd Registered in England and Wales Registered Number: 1072954 Registered office: Mortimer House, 37-41 Mortimer Street, London W1T 3JH, UK



## International Reviews in Physical Chemistry

Publication details, including instructions for authors and subscription information:

<http://www.informaworld.com/smpp/title~content=t713724383>

### Crossed-beam investigations of state-resolved collision dynamics of simple radicals

Kopin Liu<sup>a</sup>; R. Glen Macdonald<sup>a</sup>; Albert F. Wagner<sup>a</sup>

<sup>a</sup> Chemistry Division, Argonne National Laboratory, Argonne, Illinois, USA

**To cite this Article** Liu, Kopin , Macdonald, R. Glen and Wagner, Albert F.(1990) 'Crossed-beam investigations of state-resolved collision dynamics of simple radicals', *International Reviews in Physical Chemistry*, 9: 2, 187 – 225

**To link to this Article:** DOI: 10.1080/01442359009353246

**URL:** <http://dx.doi.org/10.1080/01442359009353246>

PLEASE SCROLL DOWN FOR ARTICLE

Full terms and conditions of use: <http://www.informaworld.com/terms-and-conditions-of-access.pdf>

This article may be used for research, teaching and private study purposes. Any substantial or systematic reproduction, re-distribution, re-selling, loan or sub-licensing, systematic supply or distribution in any form to anyone is expressly forbidden.

The publisher does not give any warranty express or implied or make any representation that the contents will be complete or accurate or up to date. The accuracy of any instructions, formulae and drug doses should be independently verified with primary sources. The publisher shall not be liable for any loss, actions, claims, proceedings, demand or costs or damages whatsoever or howsoever caused arising directly or indirectly in connection with or arising out of the use of this material.

## **Crossed-beam investigations of state-resolved collision dynamics of simple radicals**

by KOPIN LIU, R. GLEN MACDONALD and ALBERT F. WAGNER

Chemistry Division, Argonne National Laboratory,  
Argonne Illinois 60439, U.S.A.

A critical survey is given of new developments in the study of collision dynamics of diatomic radicals. The impetus for this survey comes from new experimental results on near state-to-state scattering dynamics of radicals with simple collision partners that have been obtained using the crossed-beam technique. These results, on both inelastic and reactive scattering, provide a unique opportunity to compare experimental observations with formal quantum scattering theory. Photodissociation is also briefly discussed because of its relevance to our fundamental understanding of fine-structure effects associated with radicals arising in all three processes. A few basic concepts pertaining to the dynamics of open-shell systems are outlined. The emphasis is on the underlying physical principles rather than on detailed theoretical treatments. To illustrate the strong interaction between theory and experiment a few case studies of systems investigated under crossed-beam conditions are highlighted. These new results also prompt an appraisal of what an experimentalist should be most anxious to measure and indicate specific areas in which further theoretical developments can be most profitable in the future.

### **1. Introduction**

Macroscopic phenomena such as combustion, plasma and atmospheric chemistry are complicated and governed by many elementary processes which occur via atomic and molecular collisions. Collisions can be divided into three broad categories: elastic, inelastic and reactive. For small systems and at low collision energies, elastic collisions normally predominate and only a change in the direction of the relative velocity of the colliding partners occurs leaving their internal energy and quantum states unchanged. Thus, elastic scattering involves an interchange of translational energy only and is primarily responsible for the macroscopic properties of diffusion, viscosity and thermal conductivity corresponding to mass, momentum and kinetic energy transfer respectively. Inelastic collisions are those involving energy transfer between the internal modes, namely electronic, vibrational and rotational degrees of freedom, of the colliding partners. Reactive collisions comprise those in which a chemical transformation occurs. Knowledge of all three types of collisions is required if the details of a chemical process are to be successfully interpreted, though in this article attention will be directed to the latter two; the inelastic and reactive ones.

Traditionally, chemists have focused on the kinetic aspects of these elementary processes by measuring overall rate constants as a function of temperature and pressure. By virtue of the nature of these experiments, the measured rate constant is a highly averaged quantity over the Maxwell-Boltzmann distributions of many individual events. Because an elementary process is fundamentally a mechanical event, involving energy transfer and/or atomic or molecular rearrangement during an individual encounter, the detailed information as to how this occurs simply cannot be inferred from such a highly averaged quantity. During the past few decades, with the

advent of more sophisticated experimental techniques, notably the crossed molecular beam and laser spectroscopic techniques, emphasis in the field has shifted from kinetic to dynamic study in which the Boltzmann average is removed and the microscopic nature of the process is revealed on the state-to-state level of detail.

In consort with experimental advances, tremendous progress has also been made in our theoretical description of these processes. The interplay of the state-resolved experimental studies and detailed theoretical calculations, in conjunction with chemical intuition, have resulted in many familiar concepts in our basic understanding of chemical dynamics. For example, a vibrational energy transfer process can often be described in terms of a simple forced harmonic oscillator model (Gentry 1979), whereas rotational energy transfer is closely related to the anisotropy of the potential energy surface (PES) (Buck 1986). For a reactive collision there is a classification of direct and complex reaction dynamics (Herschbach 1987, Lee 1987) and the effects of the late and early reaction barrier on the energy disposal (Polanyi 1972, 1987). Through the application of microscopic reversibility, much insight can be gained into the selectivity in energy consumption, that is into which form of energy (electronic, vibrational, rotational or translational) will be more effective in driving a reaction to completion. Numerous books are available on these subjects (Levine and Bernstein 1987, Smith 1980). A number of excellent reviews, both theoretical (Bernstein 1979) and experimental (Scoles 1988), are of special relevance. The reader is referred to these references, among many others, for details.

However, to date much of our basic understanding of collision dynamics implicitly assumes the validity of the Born–Oppenheimer (BO) approximation, with which a collision process is envisaged to occur with the nuclear motion evolving on a single PES. On the other hand, the vast majority of collisional processes have at least one of the reactants or products as an open-shell atom or radical. The unpaired electrons endow radicals with various fine-structure energy levels generated by the unquenched electron orbital and spin angular momenta. One may be struck by how dramatically the spectroscopic information on radicals differs from that for ordinary closed-shell molecules. In the past several years there has been an increasing awareness that the radical product fine-structure state distribution also provides a unique role in elucidating the collision dynamics. This is because in the case of a  $^{2S+1}\Sigma$  radical the coupling of the nuclear rotation and spin angular momenta will split each rotational level into several spin multiplets. For a non- $\Sigma$  radical, in addition to spin–orbit splittings, there is further splitting, a  $\Lambda$ -doublet, arising from the electron orbital–nuclear rotational couplings. Intuitively, the spin-multiplet selectivity can be regarded as a preferential alignment of the electron spin relative to some internal axis, whereas the  $\Lambda$ -doublet selectivity corresponds to a preferential spatial alignment of the electronic orbitals. Thus, the preferential fine-structure distribution in a collisional process may provide invaluable vectorial information as to the detailed dynamics involved.

Though the intuitive notion just described seems simple, the precise theoretical description as to the origin of the fine-structure selectivity for a collisional process can be quite complicated. In particular, for a scattering process involving a radical with  $\Lambda \neq 0$ , the lifting of the electronic degeneracy as a result of the interaction with the collision partner leads to the possibility that more than a single adiabatic PES and the non-adiabatic couplings among them need to be considered in describing the collision dynamics. This coupling is expected to be particularly important for states which are asymptotically degenerate. Clearly these couplings could have profound effects on the

radical product state distributions because at long range the non-adiabatic couplings can exceed the separations between the near-degenerate molecular states.

Despite these complications, we have witnessed in recent years tremendous progress in our ability to describe, in a fully quantum mechanical manner, the inelastic scattering of systems involving simple radicals. From the formal quantum analysis a number of general propensity rules, independent of the particular system being studied, have been derived. The combination of these theoretical advances and ever more detailed experimental results has considerably increased our physical insight into the nature of inelastic scattering on multiple PESs. In contrast to this, for reactive scattering, very little is known conceptually on how to properly account for the presence of multiple PESs and how to envisage the physical origin of the subsequent dynamics. However, it is also this very nature of radicals, arising from unpaired electrons, that places radicals in a unique and significant role in the overwhelming majority of chemical reactions.

Rather than providing an encyclopaedic compilation of hundreds of related works on radical dynamics, it is our intent to present a view of recent progress by focusing on a few case studies with the hope that some simple physical idea may emerge about the dynamics of open-shell systems. As will be illustrated in this article, by properly factoring out the fine-structure effect from that of the rovibrational levels, many of the concepts derived from the dynamics of closed-shell systems can still be applied to the open-shell systems. By recognizing that the fine-structure effect is intrinsically a non-adiabatic phenomenon due to the breakdown of the BO approximation, a conceptual framework emerges as to the physical interpretation of fine-structure state distributions from a reactive scattering, photodissociation as well as inelastic processes. From this viewpoint, it becomes apparent that the product fine-structure state distributions from a reactive collision often provide a unique fingerprint of the dynamics in the transition state region. This aspect is particularly exciting in view of the potential impact it might have in furthering our fundamental understanding of chemical reactivity by probing the transition state in a sensitive manner.

This article is organized as follows. In section 2 a brief remark is made regarding the experimental techniques for the state-resolved, crossed-beam scattering measurements. The inelastic scattering of simple radicals is reviewed in section 3. Some basic concepts will be first introduced, followed by a few examples for illustration. The reactive scattering is discussed in a similar fashion in section 4. Section 5 concludes with our views of the future directions. Being experimentalists, the emphasis of this article is on experimental results. However, with the recent theoretical developments, useful predictions of inelastic collision dynamics are currently being made. It is, therefore, becoming increasingly important for the experimentalist to appreciate the underlying principles governing the chemical dynamics and to distinguish them from the quantitative details associated with particular systems. With this in mind, we also attempt to extract some basic physical ideas from the esoteric mathematics and to present them in a less rigorous manner, with the hope that these perhaps oversimplified concepts still have some general validity and can be used to guide our future experiments.

## 2. Remark on experimental technique

It is not our intent to get into experimental details which are best referred to the original papers. For excellent discussions on the fundamental principles and state-of-art developments in the molecular beam technique, a recent book edited by Scoles

(1988) is highly recommended. Here, we merely want to concentrate on two aspects which are most relevant to the theme of this article.

### 2.1. Radical beam source

Supersonic beams are now widely used as sources in many spectroscopy and scattering experiments. While the production of beams of stable species presents little difficulty, the generation of a beam of transient species, in particular the molecular free radical, suitable for a scattering experiment is still a formidable task. During the past decade a variety of techniques have been developed for the generation of supersonic radical beams. These include photolysis, pyrolysis, discharge, chemical reaction, laser vapourization and combinations of these different methods. Table 1 lists some examples of simple radicals which have been successfully generated in supersonic beams. Though

Table 1. Examples of supersonic beams of transient radicals. Note: C=continuous beam; P=pulsed beam.

Radical		Method of production	Reference
<i>Source development</i>			
NH(A <sup>3</sup> Π)	C	discharge (NH <sub>3</sub> )	Carrick and Engelking (1984)
OH(X <sup>2</sup> Π)	C	discharge/reaction (CH <sub>4</sub> /CO <sub>2</sub> )	Allik <i>et al.</i> (1988)
(A <sup>2</sup> Σ <sup>+</sup> )	C	discharge (H <sub>2</sub> O)	Droege and Engelking (1983)
CN(X <sup>2</sup> Σ <sup>+</sup> )	P	photolysis (BrCN)	Heaven <i>et al.</i> (1981)
SH(X <sup>2</sup> Π)	P	photolysis (H <sub>2</sub> S)	Heaven <i>et al.</i> (1981)
NH <sub>2</sub> ( $\tilde{X}^2B_1$ )	C	discharge/reaction (CF <sub>4</sub> /NH <sub>3</sub> )	Farthing <i>et al.</i> (1983)
HCCS( $\tilde{X}^2Π$ )	C	pyrolysis (thiadiazole)	Dunlop <i>et al.</i> (1988)
<i>Spectroscopy</i>			
C <sub>2</sub> ( $\tilde{c}^3Σ_u^+ / \tilde{a}^3Π_u$ )	P	photolysis (toluene)	Van de Burgt and Heaven (1987)
( $\tilde{a}^3Π_u$ )	P	laser vapourization (graphite)	Naulin <i>et al.</i> (1988)
S <sub>2</sub> (X <sup>3</sup> Σ <sub>g</sub> <sup>-</sup> )	P	photolysis/reaction (H <sub>2</sub> S)	Heaven <i>et al.</i> (1984)
(X <sup>3</sup> Σ <sub>g</sub> <sup>-</sup> )	C	pyrolysis (sulphur)	Matsumi <i>et al.</i> (1984)
CH <sub>2</sub> ( $\tilde{a}^1A_1$ )	P	photolysis (CH <sub>2</sub> CO)	Monts <i>et al.</i> (1980)
CCl <sub>2</sub> ( $\tilde{X}^1A_1$ )	C	pyrolysis ((CH <sub>3</sub> ) <sub>3</sub> SiCCl <sub>3</sub> )	Clouthier and Karolczak (1989)
NH <sub>2</sub> ( $\tilde{X}^2B_1$ )	C	photosensitized reaction (Hg/NH <sub>3</sub> )	Mayama <i>et al.</i> (1984)
( $\tilde{X}^2B_1$ )	P	photolysis (NH <sub>3</sub> )	Curl <i>et al.</i> (1989)
HNO( $\tilde{X}^1A'$ )	C	photosensitized reaction (Hg/H <sub>2</sub> /NO)	Obi <i>et al.</i> (1983)
CH <sub>3</sub> ( $\tilde{X}^2A''$ )	P	pyrolysis ( <i>t</i> -butyl nitrite)	Chen <i>et al.</i> (1986)
<i>Scattering</i>			
CH(X <sup>2</sup> Π)	P	photolysis (CH <sub>3</sub> I)	Macdonald and Liu (1989)
NH(X <sup>3</sup> Σ <sup>-</sup> )	P	photolysis (NH <sub>3</sub> )	Dagdigian (1989b)
( <i>a'</i> Δ)	P	photolysis (HN <sub>3</sub> )	Sauder <i>et al.</i> (1989)
OH(X <sup>2</sup> Π)	P	photolysis (HNO <sub>3</sub> )	Andresen <i>et al.</i> (1984)
NH <sub>2</sub> ( $\tilde{X}^2B_1$ )	P	photolysis (NH <sub>3</sub> )	Dagdigian (1989a)
CH <sub>3</sub> ( $\tilde{X}^2A''$ )	C	pyrolysis (di- <i>t</i> -butyl peroxide)	Robinson <i>et al.</i> (1988)
( $\tilde{X}^2A''$ )	C	pyrolysis (azomethane)	Brown <i>et al.</i> (1976)

not included in the table, it should be mentioned that there is a vast amount of work on transient atomic species (Scoles 1988). For large molecular radicals and ions several review articles by Miller (1982, 1984) and by Foster and Miller (1989) are recommended. Finally, the laser vapourization technique developed by Dietz *et al.* (1981) and independently by Bondybey and English (1981) has recently become the workhorse for the generation of a variety of metal and semiconductor clusters. The choice of method certainly depends on the individual case. Nevertheless, some guidelines can be given based upon the following considerations. It should be noted that in practice the following criteria are sometimes conflicting to one another and in such cases a compromise will be necessary.

### 2.1.1. Intensity

This is perhaps the most important consideration for a scattering experiment because of the potential loss due to the high reactivity of transient radicals. To appreciate this, let us consider a state-resolved, crossed-beam scattering experiment. To make a clear connection with the experiments to be discussed later, both beams are assumed to be in the pulsed form and the radical is generated by a photolytic method of an appropriate precursor during the supersonic expansion. A typical skimmed pulsed molecular beam will yield an instantaneous intensity corresponding to a density of  $\sim 3 \times 10^{13}$  molecules  $\text{cm}^{-3}$  at the scattering centre  $\sim 10$  cm away from the nozzle. If a 1% seeding ratio is assumed for the precursor to the expansion carrier gas and a nominal conversion efficiency of a few per cent is taken for the generation of radical species after accounting for the photolysis quantum-efficiency, the reaction loss of radicals during the expansion and the escape of the radicals from the main stream of the beam, then the beam intensity will be of the order of  $10^{10}$  radicals  $\text{cm}^{-3}$  at the scattering centre. For a reaction cross-section of  $1 \text{ \AA}^2$  and a typical 6 mm beam width for the target beam, the fraction of radicals which undergo reaction is  $10^{-3}$  or the total product yield becomes  $1 \times 10^7$  molecules  $\text{cm}^{-3}$ . For the geometry considered here this corresponds to  $\sim 2 \times 10^6$  molecules. If a total of 30 product states can be populated, then an average of  $6 \times 10^4$  product molecules per quantum state is expected. Clearly, an intense radical beam and a very sensitive state-specific detection scheme are essential in this kind of experiment.

### 2.1.2. Purity

By virtue of the transient characteristics of free radicals, it is necessary that they are produced *in situ*. From a simple mass-balance consideration, generating a given radical is often accompanied with some other reactive species or the same radical but in undesired metastable electronic states. Though this may be a welcome situation for spectroscopic work, it could be a serious problem for a reactive scattering experiment because of the potential chemical interferences from those undesired radicals. Unfortunately, there is no general solution to this problem, which is best handled on an individual basis. Energetic considerations can be useful in eliminating some of the possibilities, but often not all of them. In the reactive scattering study of  $\text{CH} + \text{D}_2$  (Macdonald and Liu 1990b), the  $\text{H}_2$  molecule was deliberately chosen as the main carrier gas for the CH radical beam with this problem in mind. Any reactive species other than CH which could react with  $\text{D}_2$  at the collision centre to produce CD was removed from the primary beam by reaction with  $\text{H}_2$  during the supersonic expansion. In other words, the supersonic expansion not only served to cool the photolysed CH radical, but also acted as a chemical 'pre-reactor' to clean up the primary beam in that case.

### 2.1.3. Cooling

Although a supersonic expansion is recognized as a means of generating cold gas phase molecules, the demand for cooling is far more stringent for a cold radical beam because the radical is often produced initially with high internal excitation. Unlike the chemical purity consideration which is more problematic for reactive scattering experiments than for inelastic ones, the cooling (or state purity) requirement reverses for the two processes. The trick of achieving a cold supersonic beam is still a black art. To generate a beam cold enough for the experiment but without clustering makes this requirement even more challenging.

The use of pulsed laser photolysis (or vapourization) with a pulsed molecular beam valve for generating a radical beam has gained considerable popularity in recent years. This approach not only allows optimum use of the available apparatus gas throughput, but also matches perfectly with the pulsed laser spectroscopic techniques such as LIF and REMPI for the state-specific product detection (Gentry 1988). To our best knowledge, this is also the only approach that has been successfully employed in state-resolved, crossed-beam scattering experiments to date. Because this approach may not be the ideal one for generating all radicals, the further development of other methods, such as those exemplified in table 1, for state-resolved scattering experiments will be extremely desirable.

### 2.2. Detection: number density, flux or something else?

A laser-based detection scheme is clearly the method of choice for a state-to-state scattering experiment. The quantity measured by laser spectroscopy techniques is the total number of molecules in a specific quantum state within the detection volume, which does not necessarily correspond to the product flux, the desirable quantity in a scattering experiment. When it is used to monitor the nascent product state distribution and thus to deduce the state-resolved cross-section or rate constant, the question of number density or flux detection arises. Under favourable conditions, either the kinematic constraints are such that the number density–flux transformation is not a large correction to the data or the experimental geometric arrangements are such that a flux mode of detection can be realized; thus, a direct comparison with theoretical calculations can be made with confidence. However, in general, this is not the case. While this problem has been pointed out in the past and well recognized in the field (Dagdigian 1988, Hefter and Bergmann 1988), little attention has been paid to it in practice. This is perhaps because the density-to-flux transformation depends on the laboratory velocity of the product in a specific quantum state and so requires a knowledge of the state-specific differential cross-sections, which are generally lacking in the state-resolved integral cross-section measurements. Nevertheless, this problem deserves more attention, particularly it has been clearly shown (Macdonald and Liu 1989a) that improper analysis of experimental data can lead to anomalous results which could mistakenly be taken as some dynamical effect of the process under study. In this regard, the model recently proposed by Naulin *et al.* (1988), which fully accounts for this transformation, is particularly significant.

In the course of an investigation of the inelastic scattering of OH + CO and N<sub>2</sub> in our laboratory the problem of density–flux transformation rose. A general, but not perfect, scheme (Sonnenfroh *et al.* 1990) was then developed to determine the transformation experimentally. The basic idea of the analysis lies upon the fact that the transformation depends on the dynamics as well as the kinematics. The former are the initial collision energy and product state-specific differential cross-section, whereas the

latter are experimental geometric factors, such as the beam dimensions, pulse duration and Newton diagram. If one can perform the experiments under different kinematic but identical dynamical conditions, then the results from these independent measurements will give the necessary conversion factor because the integral cross-section should be invariant with the experimental geometric arrangements. The result of this approach is illustrated in figure 1. The experiments were performed by taking advantage of the flexibility of the Gentry–Giese style (i.e. rotating sources) crossed-beam apparatus (Hall *et al.* 1984, Macdonald and Liu 1989). By varying the initial beam velocity the same collision energy can be achieved with completely different intersection angles between the two molecular beams. Knowing the experimental geometric arrangements and with the aid of a simple model the conversion factor for the transformation can be deduced.

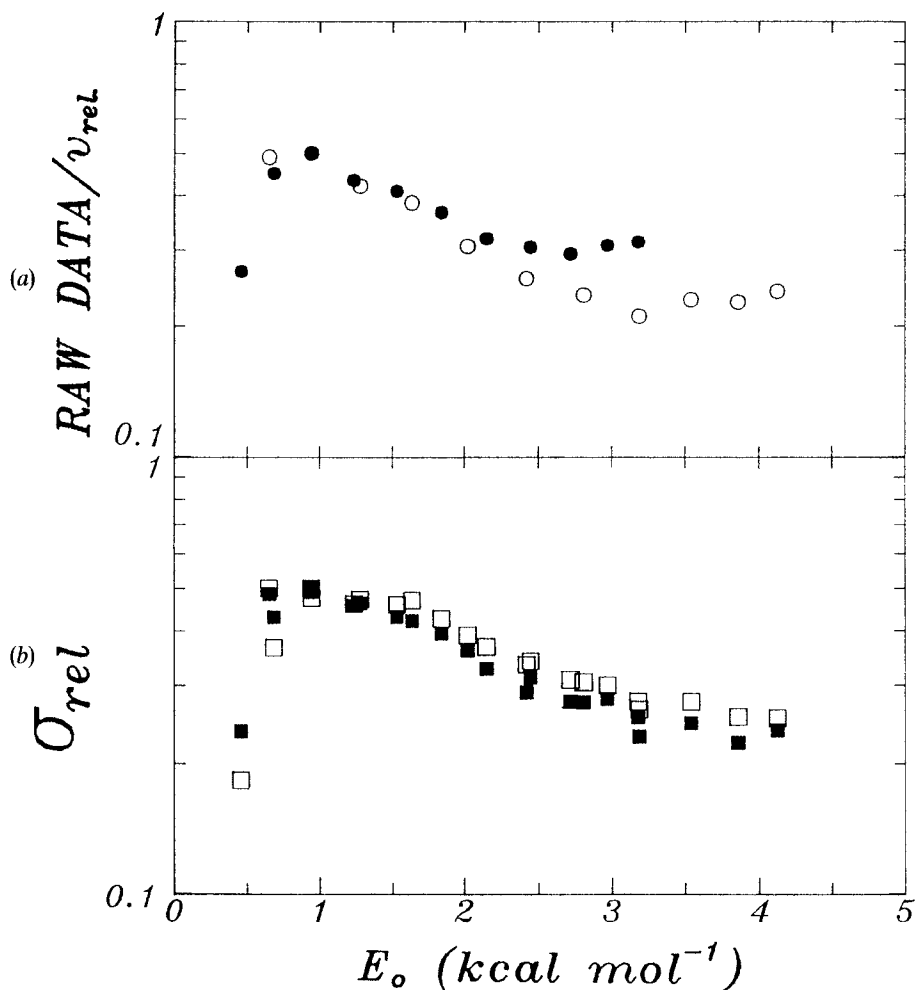


Figure 1.  $\text{OH}(^2\Pi_{3/2}, J=3/2) + \text{CO} \rightarrow \text{OH}(^2\Pi_{1/2}, J'=1/2) + \text{CO}$ . (a) The signal intensity divided by the relative velocity obtained under two different kinematic conditions ( $\circ$   $v_{\text{OH}} = 1.07 \times 10^5 \text{ cm s}^{-1}$  and  $\bullet$   $v_{\text{OH}} = 0.84 \times 10^5 \text{ cm s}^{-1}$ ). (b) The density-to-flux transformation corrected excitation functions from the data shown in (a) for two extreme assumptions about the angular distribution for this state ( $\blacksquare$  backward and  $\square$  forward scattering). From Sonnenfroh *et al.* (1990).



Because all parameters in the model are easily determined from the experiments and are not allowed to be adjusted, the agreement in the results (figure 1(b)) is taken as strong support for this approach. Also indicated in figure 1(b) are the results from assuming two limiting angular distributions. As can be seen, the two distributions give a nearly identical shape for the excitation function. Thus, though this scheme is able to yield the correct shape of the excitation function, it fails to distinguish between the two angular distributions for this particular case because of the unfavourable kinematic constraint and signal-to-noise ratio requirement.

### 3. Inelastic scattering

#### 3.1. Some basic concepts

Over the last fifteen years there has been a wealth of detailed information on the inelastic scattering of closed-shell molecules ( $^1\Sigma$ ) with closed-shell atoms or molecules (Brunner and Pritchard 1982, Buck 1986, Schinke 1986). There are even available state-resolved differential cross-section measurements for inelastic energy transfer processes (Jones *et al.* 1983). The theoretical advancements in this field have been as impressive as the experimental ones and we now have a rather complete understanding of rotational energy transfer between closed-shell diatomic molecules and closed-shell atoms or molecules (Kouri 1979, Secrest 1979, Schinke and Bowmann 1983). For this case the PES, represented by  $V(\mathbf{R}, \mathbf{r}, \gamma)$ , depends on three variables usually taken as the position vector  $\mathbf{R}$ , between the centre-of-mass of the diatom and the atom, the internuclear separation vector  $\mathbf{r}$  of the diatom and the orientation angle between these two vectors,  $\gamma$ . Roughly speaking, the dependence of  $V(\mathbf{R}, \mathbf{r}, \gamma)$  on  $\mathbf{r}$  and  $\gamma$  induce vibrational and rotational transitions respectively, whereas the  $\mathbf{R}$  dependence of  $V(\mathbf{R}, \mathbf{r}, \gamma)$  determines the angular distributions of the measured quantities.

The two most common time-independent formulations of the quantum scattering theory of a closed-shell ( $^1\Sigma$ ) molecule and a closed-shell ( $^1S$ ) atom are that by Arthurs and Dalgarno (1960) who described the collision in a space-fixed coordinate system and that by Curtiss *et al.* (1950) who used a body-fixed coordinate system to describe the collision. In the space-fixed treatment, the  $z$  axis of the centre-of-mass coordinate system remains fixed in space during the collision, while in the body-fixed treatment, the  $z$  axis is rotated so that it lies along the direction of  $\mathbf{R}$  throughout the collision. Though both formulations are exact (Pack 1974), considerable physical insight can be obtained from the body-fixed treatment. In this formulation, rotational excitation for a short-range anisotropic PES can be viewed as a three-stage process. First, as the atom approaches, a coriolis force is exerted on the molecule due to the long-range centrifugal potential resulting in a reorientation of the rotational angular momentum ( $\mathbf{j}$ ); the projection of  $\mathbf{j}$  on the body-fixed  $z$  axis ( $j_z$ ) changes, represented by  $(\mathbf{j}, j_z) \rightarrow (\mathbf{j}, j_z')$ . Second, as the classical turning point is approached, the atom exerts a torque on the diatom as determined by the rotational coupling matrix element. In the body-fixed frame this torque causes a change in  $\mathbf{j}$  but not in  $j_z$ ; the transition  $(\mathbf{j}, j_z) \rightarrow (\mathbf{j}', j_z)$  is made. Finally, as the atom recedes, it again exerts a coriolis force to reorientate  $\mathbf{j}'$ ;  $(\mathbf{j}', j_z) \rightarrow (\mathbf{j}', j_z')$ . The change in orientation of  $\mathbf{j}$  (or polarization effects) in the initial and final stages of the collision is classically equivalent to a change of the plane of rotation of the molecule with respect to the position vector  $\mathbf{R}$ .

This description is somewhat over-simplified because the coriolis coupling can also be present at short range. In particular, if the PES is relatively anisotropic at long range, then this simple view may not be valid and no clear partitioning of the effects of different

parts of the PES is possible. Nevertheless, the description of rotational energy transfer roughly as a three-stage process suggests that if only  $\Delta j$  transitions are of interest, then a good approximation to the body-fixed, close-coupling equations can be obtained by diagonalizing the centrifugal potential coupling, that is completely neglecting the couplings in  $j_z$  (the so-called  $j_z$ -conserving, centrifugal-sudden (or coupled-states) (CS) approximation (McGuire and Kouri 1974)). Under these circumstances, the degeneracy-averaged rotational energy transfer cross-sections can be related to the short-range anisotropic parts of the PES.

Within the CS approximation, rotational energy transfer for closed-shell systems can be roughly classified into three rather broad categories. This categorization essentially depends on the strength of the coupling between the rotational and translational degrees of freedom, or the anisotropy of the PES, as weak, moderately strong and extreme, and according to the ratio of the translational energy  $E_0$  to the rotational constant  $B$  (i.e.  $E_0/B$ ). For light diatoms with large  $B$  such as HD–He at thermal energies  $E_0/B$  is small ( $< 10$ ) and the collision dynamics are dominated by elastic scattering and the cross-sections for rotational energy transfer to the few energetically accessible rotational states are small. When  $E_0/B$  is large ( $> 1000$ ), such as Na<sub>2</sub>–inert gas, the collision is impulsive in nature and the dynamics are dominated by inelastic scattering which can often be characterized by rotational rainbow features. These rotational rainbow features of the collision dynamics are most easily seen as pronounced structures in state-resolved differential cross-section measurements; however, they can also manifest themselves in state-resolved integral cross-section measurements. A useful concept that has emerged from these studies is the hard-shell model. In this model the rotational rainbow curve  $j_R(\theta)$  is given by

$$j_R(\theta) = -2k \left. \frac{\partial \mathbf{R}(\gamma)}{\partial \gamma} \right|_{\gamma_R} \sin(\theta/2) \quad (1)$$

where the potential  $V(\mathbf{R}, \mathbf{r}, \gamma)$  is approximated by a hard-shell with contour  $\mathbf{R}(\gamma)$ ,  $k$  is the wavenumber for the collision and  $\theta$  is the scattering angle. The usefulness of equation (1) is that identification of  $j_R(\theta)$  gives direct information on the anisotropy of the PES, sometimes in an almost quantitative fashion. The third category is the case of extreme translation–rotation coupling and is exemplified by multiple collision rainbows. This phenomenon is expected to occur in collisions between heavy collision partners with very anisotropic PES when almost all the initial translational energy has been transferred into rotational energy at the classical turning point of a trajectory. Because of the heavy mass of the collision partners, the departing translational velocity is small and secondary contacts occur transferring part of rotational energy back into translational energy. This process can lead to more than a single rotational rainbow feature. An excellent example of this class of inelastic collision dynamics is the CO<sub>2</sub> + Xe system (Buch *et al.* 1985).

In contrast to the situation for collisions between closed-shell partners, the collision dynamics of open-shell systems has not been so systematically characterized, though significant progress has been made as indicated in table 2. Part of the difficulty in dealing with the collision dynamics of open-shell systems is the intrinsically complicated description of rotational energy levels of isolated open-shell molecules themselves. Each rotational level is split into several fine-structure states because of the interaction of the nuclear rotational motion with the electronic degree of freedom. The proper description of these quantum states is provided by various Hund's case coupling schemes. Hence, it is not clear *a priori* how to extend the concepts of closed-shell

Table 2. Examples of some of the fine-structure propensity rules for inelastic scattering of diatomic radicals within a single electronic state.

Collision system	Propensity observed	Reference
OH(A <sup>2</sup> Σ <sup>+</sup> , e, f) + Ar, H <sub>2</sub> , N <sub>2</sub>	e→e and f→f	Lengel and Crosley (1977) Stepowski and Cottreau (1981)
BaF(B <sup>2</sup> Σ <sup>+</sup> , e, f) + Ar	e→e, f→f	Ip <i>et al.</i> (1981)
CaCl(X <sup>2</sup> Σ <sup>+</sup> , e) + CH <sub>3</sub> Cl	e→e	Dagdigian and Bullman (1984)
CaCl(X <sup>2</sup> Σ <sup>+</sup> , e) + HCl, HCN, SO <sub>2</sub>	e→e	Dagdigian and Bullman (1985)
CaCl(X <sup>2</sup> Σ <sup>+</sup> , e) + NO	e→e	Corey <i>et al.</i> (1986)
CaCl(X <sup>2</sup> Σ <sup>+</sup> , e) + Ar	e→e	Alexander <i>et al.</i> (1985a)
S <sub>2</sub> (B <sup>3</sup> Σ <sub>g</sub> <sup>-</sup> , F <sub>1</sub> ) + He, Ar, Xe	F <sub>1</sub> →F <sub>1</sub>	Caughy and Crosley (1979)
NH(X <sup>3</sup> Σ <sup>-</sup> , F <sub>1</sub> ) + Ar	F <sub>1</sub> →F <sub>1</sub>	Dagdigian (1989b)
Na <sub>2</sub> (B <sup>1</sup> Π <sub>u</sub> ) + noble gases, H <sub>2</sub>	σ <sub>j</sub> (+Δj)/σ <sub>j</sub> (-Δj) asymmetric	Bergmann and Demtroder (1971) Bergmann and Demtroder (1972) Al-Imarah <i>et al.</i> (1984)
Li <sub>2</sub> (B <sup>1</sup> Π <sub>u</sub> ) + noble gases	σ <sub>j</sub> (+Δj)/σ <sub>j</sub> (-Δj) asymmetric	Ottinger <i>et al.</i> (1970) Ottinger and Poppe (1971) Lemoine <i>et al.</i> (1987)
OH(X <sup>2</sup> Π <sub>3/2</sub> , e=f) + H <sub>2</sub>	Π(A') > Π(A'')	Andresen <i>et al.</i> (1984)
OH(X <sup>2</sup> Π <sub>3/2</sub> , e=f) + CO, N <sub>2</sub>	Π(A') > Π(A'')	Sonnenfroh <i>et al.</i> (1990)
NO(X <sup>2</sup> Π <sub>1/2</sub> , e=f) + He, Ne, Ar	Ω <sub>1/2</sub> →Ω <sub>1/2</sub> Ω <sub>1/2</sub> →Ω <sub>3/2</sub> weak	Joswig <i>et al.</i> (1986a)
CH(X <sup>2</sup> Π <sub>1/2</sub> , e=f) + He, D <sub>2</sub>	Π(A'') > Π(A')	Macdonald and Liu (1989, 1990a)
CaF(A <sup>2</sup> Π, f) + He, Ar	f→f	Dufour <i>et al.</i> (1985)
ZnH(A <sup>2</sup> Π, e, f) + He, Ar	e→e, f→f slight	Nedelec and Dufayard (1984)
CdH(A <sup>2</sup> Π, e, f) + He, Ar	e→e, f→f dominate	Nedelec and Dufayard (1985)
N <sub>2</sub> (B <sup>3</sup> Π <sub>g</sub> ) + Ar	F <sub>1</sub> →F <sub>1</sub> , ΔJ even	Ali and Dagdigian (1987)

collision dynamics to these open-shell systems. For example, in inelastic collisions between <sup>1</sup>Σ diatomic molecules and spherically symmetric collision partners the translational motion of the collision partners is only coupled to the nuclear rotational degree of freedom; for similar collisions involving radicals, translation can be coupled to the various internal angular momenta and the collision can be *elastic* with respect to nuclear rotation but *inelastic* with respect to the electronic degrees of freedom. As a further complication, the Hund's case description of the open-shell diatom can also be a function of the rotational energy with a gradual transition from case (a) to case (b) and finally, towards case (d) as the rotational quantum number increases (Herzberg 1950).

Despite these complications, the theoretical foundation laid down by Alexander and co-workers allows for a rigorous treatment of the collision dynamics of open-shell diatomic molecules and provides physical insight into this process. Owing to the limited scope of this article, only inelastic processes within a single electronic state of the diatom will be considered. Thus collision-induced electronic-to-electronic energy transfer will not be reviewed here. The collision dynamics of transient diatoms with a structureless particle can be divided into two classes, those radicals that do not possess

electronic orbital angular momentum; for which the projection of the electronic angular momentum along the internuclear axis,  $A$ , is zero in which case the electronic state of the radical is specified by  $^{2S+1}\Sigma$ , and those radicals for which  $A \neq 0$  and the electronic state is given by  $^{2S+1}\Lambda$ . For brevity, we will only highlight some of the basic concepts from the rigorous theoretical treatments.

### 3.1.1. $^{2S+1}\Sigma$ radicals

Almost all  $^2\Sigma$  diatomic radicals are described by Hund's case (b) coupling and the spin  $\mathbf{S}$  is only weakly coupled to the rotational angular momentum  $\mathbf{N}$ , resulting in a splitting of each rotational level into spin doublets. The corresponding parallel and anti-parallel coupling of  $\mathbf{N}$  and  $\mathbf{S}$  are labelled by e and f for a  $^2\Sigma^+$  and the reverse for a  $^2\Sigma^-$  electronic state respectively (Brown *et al.* 1975). The PES governing a collision between a  $^2\Sigma$  radical and a structureless target is assumed to be purely electrostatic in nature so that  $\mathbf{S}$  cannot be directly influenced by the collision. The effect of the collision is to cause a change in both the magnitude and/or direction of  $\mathbf{N}$ . Thus, the spin can be treated as a spectator during the collision, because  $\mathbf{N}$  and  $\mathbf{S}$  are weakly coupled. The only effect of the collision on  $\mathbf{S}$  is to change the direction of its quantization axis. In other words, collision-induced transitions between spin doublets (i.e. e $\leftrightarrow$ f) can occur only through a change in the final  $\mathbf{N}$ - $\mathbf{S}$  precession angle. Guided by this intuitive collision mechanism, Corey and McCourt (1983) proposed an angular momenta recoupling scheme to treat, within an exact quantum mechanical formalism, the inelastic scattering between a Hund's case (b)  $^{2S+1}\Sigma$  radical and a  $^1S$  atom. This recoupling scheme can be represented vectorially by

$$\mathbf{N} + \mathbf{l} = \mathbf{j}; \quad \mathbf{j} + \mathbf{S} = \mathbf{J}, \quad (2)$$

where  $\mathbf{l}$  is the orbital angular momentum of the collision partners and  $\mathbf{J}$  is the total angular momentum of the system. One way of viewing the recoupling scheme (2) is that the open-shell dynamical problem is reduced to the collision of a molecule without electron spin, with the intermediate angular momentum  $\mathbf{j}$  playing the same role as the total angular momentum in the case of a collision of a closed-shell diatom. Thus, rigorously, from the formal description of the collision dynamics the interaction potential matrix elements can be separated into a purely geometrical factor, which depends on the spin and a purely dynamical factor, which describes the evolution of the nuclear motion over a potential energy surface appropriate to a collision between a  $^1\Sigma$  molecule and a  $^1S$  atom. However, the scattering amplitude describing the final state product distribution cannot be so simply factored because the total molecular angular momentum  $\mathbf{N} + \mathbf{S}$  is coupled to the total angular momentum of the system  $\mathbf{J}$ . Nevertheless, if the final spin states of the rotational energy transfer are not resolved, then the collision dynamics can be treated exactly as for a  $^1\Sigma$  molecule and a  $^1S$  atom. This result is independent of any dynamical approximation and is valid at the close-coupling level of the formulation of the collision dynamics for a  $^{2S+1}\Sigma$  radical in the case (b) limit.

By combining the recoupling scheme (2) and the translational-rotational coupling scheme first introduced by Curtiss (1969), Hunter and Curtiss (1973), Hunter and Snider (1974), Alexander *et al.* (1986) were able to clearly establish the connection between the observed propensity toward conservation of the e/f symmetry label, table 2, and the collisional propensity to retain the initial orientation of  $\mathbf{N}$ . As anticipated, this propensity rule becomes stronger as the initial rotational level increases because collisions become less effective at reorientating  $\mathbf{N}$  (Derouard 1984).

Similar considerations apply to inelastic collisions between a  $^3\Sigma$  molecule and a symmetric collision partner (Corey and McCourt 1983, Alexander and Dagdigian 1983, Alexander *et al.* 1986 and Dagdigian 1989a, b). A  $^3\Sigma$  molecule can be described by either Hund's case (a) or case (b) coupling depending on whether the spin-spin coupling constant is larger or smaller than the rotational constant. For fine-structure state resolved cross-sections there is a strong propensity to remain in the initial spin manifold  $F_i$  as the initial  $J$  state increases. For a case (a) molecule there is a propensity against  $F_1 \rightarrow F_3$  transitions for all  $J$ . The validity of the propensity rules for case (b)  $^3\Sigma$  molecules has been demonstrated for  $\text{NH}(X^3\Sigma^-) + \text{Ar}$  collisions by Dagdigian (1989a, b). Again the physical reason for their occurrence is the purely electrostatic intermolecular potential and the ineffectiveness of collisions to reorientate  $\mathbf{N}$  so that the angle between  $\mathbf{N}$  and  $\mathbf{S}$  tends to be preserved in collisions. If the interaction is dominated by short-range forces and the collision energy is large compared to the energy level spacing, then the infinite-order-sudden (IOS) approximation can be applied. This leads to a considerable simplification of the cross-section expression and a factorization into simple base cross-sections (i.e. scaling law) as for the rotational energy transfer between a  $^1\Sigma$  (and  $^2\Sigma$ ) molecule and a  $^1\text{S}$  atom.

### 3.1.2. $^{2S+1}\Pi$ radicals

For radicals that possess electron orbital angular momentum the dynamics of inelastic collisions are more complicated than that for  $\Sigma$  species because the relative motion of the collision partner can couple not only with the rotational motion of the molecule, but also with the orbital motion of the unpaired electron. The interaction potential, as obtained from *ab initio* calculations, involves two adiabatic PESs of  $A''$  and  $A'$  symmetry in planar geometry. These PESs arise when the approach of a spherical partner lifts the electronic degeneracy of a radical in a  $\Pi$  electronic state. The description of the rotational energy levels of the isolated radical are also more complicated because of  $A$ -doubling phenomenon (Herzberg 1950) in which electron orbital and nuclear rotational motions are coupled removing the degeneracy of electronic states characterized by electron orbital angular momentum components  $+A$  and  $-A$  on the internuclear axis.

In a classic work, Alexander (1985) derived explicit expressions for the electrostatic potential matrix required in the quantum treatment of the collision dynamics of a  $\Pi$  molecule. More importantly, this derivation makes a clear connection between the matrix elements and the two adiabatic PESs of  $A''$  and  $A'$  symmetry. In this formalism the collision occurs on neither of these PESs, instead the average potential,  $\frac{1}{2}(V_{A''} + V_{A'})$  and the difference potential,  $\frac{1}{2}(V_{A''} - V_{A'})$ , are needed to describe the collision dynamics. The average and difference potentials arise from an application of the concept of frame transformation as follows. The interaction potentials governing the collision are defined in the body-fixed (or collision) frame while the molecular wavefunctions for a  $\Pi$  electronic state are defined in the molecular frame. A frame transformation of the interaction potential from the body frame to the molecular frame relates electrostatic potential matrix elements, which are usually expressed in terms of diabatic  $\pm A$  basis wavefunctions, to the adiabatic potentials which arise naturally from electronic structure calculations. It is this transformation which gives rise to the average and difference potentials in the quantum scattering treatments of the collision dynamics. This treatment is applicable to a  $\Pi$  state molecule with arbitrary multiplicity; however, we will concentrate mainly on the inelastic scattering of  $^2\Pi$  radicals for illustration.

Most  ${}^2\Pi$  molecules can be described by a Hund's case (a) or (b) coupling scheme (Herzberg 1950). A Hund's case (a) description is appropriate if the spin-orbit constant  $A$  is much larger than the rotational spacing (i.e.  $A \gg BJ$ ). In this limiting case  $\Lambda$  and  $\Sigma$  are strongly coupled to form

$$\Omega = |\Lambda + \Sigma|, \quad \Omega = \frac{1}{2} \text{ or } \frac{3}{2}$$

and the electron density is cylindrically symmetric about the internuclear axis. From the formal quantum analysis of the collision dynamics (Alexander 1982), it has been possible to make a number of general observations and propensity rules for the inelastic scattering of a case (a)  ${}^2\Pi$  molecule and a spherically symmetric collision partner. For example, the transitions within a spin-orbit manifold ( $\Omega$ ) are governed exclusively by the average potential, whereas transitions between spin-orbit manifolds are governed exclusively by the difference potential. This observation arises from symmetry considerations of the expansion terms of the electrostatic potential matrix elements. Under sudden limits it has also been shown that the inelastic cross-sections will be unchanged with respect to an exchange in the  $e/f$  parity labelling of the initial and final states. In other words, the cross-section for a  $Je \rightarrow J'f$  transition will be identical to that for a  $Jf \rightarrow J'e$  and similarly, for a  $Je \rightarrow J'e$  transition as compared to a  $Jf \rightarrow J'f$  transition. This implies that there will be no  $\Lambda$ -doublet preference in the inelastic product state distribution if the initial  $\Lambda$ -doublet states are equally populated. In addition, at higher  $J$ , there will be a stronger tendency to conserve the initial parity label;  $e \rightarrow e$  and  $f \rightarrow f$  transitions will be more probable than  $e \rightarrow f$  and  $f \rightarrow e$ . This propensity rule is entirely equivalent to that for collisions of  ${}^2\Sigma$  radicals and the physical origin is similar, at large  $J$  collisions become less effective at decoupling  $\Omega$  from nuclear rotation. These propensity rules have been confirmed in a number of experiments, table 2.

When  $BJ \geq A$  the radical is best described by an intermediate or case (b) coupling scheme and the  $e/f$  symmetry of the inelastic cross-sections just described is lost. The resulting asymmetry in inelastic cross-sections can be quite large. Such effects have important implications in the pumping mechanism of the astronomical OH maser (Andresen *et al.* 1984, Andresen 1986). Dagdigian *et al.* (1989) have discussed this behaviour and showed that it originates from the mixing of case (a) spin-orbit manifold wavefunctions in describing an intermediate or case (b) radical. As a result, both the average and difference potentials contribute to spin-orbit state changing as well as conserving transitions. Furthermore, interference between scattering amplitudes arising from the average and difference potentials can result in unequal  $\Lambda$ -doublet population of the product states, that is there is an  $e/f$  asymmetry in the inelastic cross-sections even when the  $\Lambda$ -doublet states of the initial rotational level are equally populated. A simple pictorial representation was proposed (Macdonald and Liu 1989) to aid in visualizing the basic difference between inelastic scattering of a Hund's case (a) and a case (b) radical with a structureless atom and how interference can arise in case (b) but not in case (a) coupling. For a  ${}^2\Pi$  Hund's case (b) radical at the high  $J$  limit, each  $\Lambda$ -doublet component can be characterized by the reflection symmetry of the electronic wavefunction with respect to the plane of rotation as either  $\Pi(A'')$  or  $\Pi(A')$  (Alexander *et al.* 1988a). Because the  ${}^2\Pi$  electronic state of most diatomic molecules comes from either a singly occupied  $\pi^1$  molecular orbital (e.g.  $\text{CH}(X^2\Pi)$  and  $\text{NO}(X^2\Pi)$ ) or a  $\pi^3$  electron occupancy (e.g.  $\text{OH}(X^2\Pi)$  and  $\text{CN}(A^2\Pi)$ ), unequal  $\Lambda$ -doublet population in product state distributions can also be viewed as preferential orbital alignment with respect to this plane.

All singlet states have no resultant spin angular momentum and so can be equally classified in terms of either case (a) or case (b) coupling. For the inelastic scattering of a  $^1\Pi$  molecule with a structureless partner, Alexander (1985) and Lemoine *et al.* (1987) have shown that its dynamical behaviour is similar to that for a  $^2\Pi$  case (b) molecule. Thus the collision dynamics are again governed by the average and difference potentials and interference between these two paths can occur. Similarly, the different propensity rules appropriate for either case (a) or case (b)  $^2\Pi$  molecules can be applied to the corresponding  $^3\Pi$  molecule (Alexander and Pouilly 1983) (but notice that there is a reversal of the electronic wavefunction symmetry for the  $F_2$  manifold in going from case (a) to case (b) coupling (Alexander *et al.* 1988a)).

The above discussion has focused primarily on propensity rules. It is also important to note that overall rovibrational inelasticity may be affected by unusual anisotropic features of the  $A'$  and/or the  $A''$  PES governing the scattering of  $^{2S+1}\Pi$  diatomic molecules. By the *closed* nature of closed-shell diatomic molecules, there is a limit to the anisotropy such systems can demonstrate. All atomic electronic orbitals are fully occupied or involved in bonding and become centres for repulsion for collision partners in non-reactive encounters. For open-shell diatomics, a greater variation in electronic orbital placement and occupation is possible. Consider  $\text{CH}(X^2\Pi)$  for example (Kok *et al.* 1990). The valence electrons in this molecule are involved in a  $\sigma$  bond, a lone pair along the bond axis, and a radical orbital either in ( $A'$ ) or out ( $A''$ ) of the plane of CH and its collision partner. The  $A'$  PES has an anisotropy typical of closed-shell systems in that any direction of approach by the collision partner will involve an encounter with an electron orbital. The basic shape of CH to the collision partner is that of a hydrogen halide: a mostly spherical contour about the heavy atom with a bump on the contour for the H atom. The  $A''$  PES, however, is completely different because the radical orbital is out of the plane which allows a very close approach of the collision partner in the direction perpendicular to the bond. The overall shape of this surface is that of a peanut. This degree of anisotropy is not attained in closed-shell hydrides unless the bond distance is considerably stretched from equilibrium. The implications for rovibrational distributions of the enhanced degree of anisotropy possible in the PES of  $^{2S+1}\Pi$  diatomic molecules is not yet clear, in part because the sum and difference of the  $A'$  and the  $A''$  PES are the operative forms in the scattering. Applying the rotational rainbow concepts (e.g. equation (1)) to derive information about the potential is complicated by the presence of two potentials which can have dramatically different levels of anisotropy. Further work in this area is required (Wagner and Alexander 1990).

The  $A'$  and the  $A''$  PESs are, generally, calculated within the context of the BO approximation. Thus electron orbit- and spin-(nuclear-rotation) operators are *not* included in the electronic structure calculation. Generally, spin-orbit operators are also ignored in the calculations. Alexander's work provides a framework within which PESs calculated without the inclusion of these operators can be combined with the coupling elements of these operators experimentally derived from the spectroscopy of the reactants. This approach has provided great insight in the scattering of open-shell species. However, it is an approximation to use *reactant* coupling elements when these elements are rigorously a function of the position of the collision partners during the scattering event. Theoretical calculations of the coupling element between surfaces are beginning to be made (Yarkony 1989a, b) but are far from routine. The positional dependence of these coupling elements can also be approached rather directly through spectroscopy of van der Waals (radical-diatom)-(rare-gas) pairs. The first observations of such clusters has recently been made (Fawzy and Heaven 1988, Berry *et al.* 1988). However to date, the spin-orbit or lambda-doublet manifolds have not been observed.

## 3.2. Specific systems

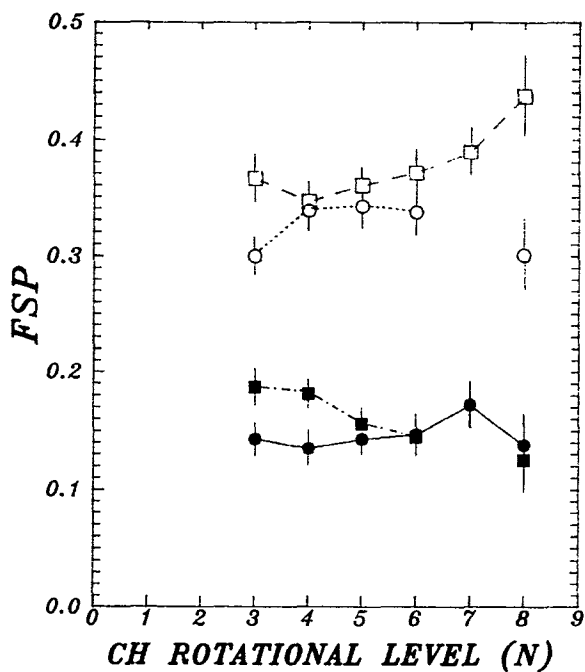
3.2.1.  $\text{CH}(X^2\Pi) + \text{He}(^1\text{S})$  and  $\text{D}_2(X^1\Sigma_g^+)$ 

In the crossed-beam experiments of Macdonald and Liu (1989, 1990a), the CH radicals were state-selected by a supersonic expansion with 93% of the population in the lowest rotational level and with equal population in the  $\Lambda$ -doublet components. The CH radical was probed in a state-specific manner using laser-induced fluorescence (LIF). Because the CH radical is an excellent example of a Hund's case (b) molecule and the  $V_{A'}$  and  $V_{A''}$  intermolecular potentials are expected and were later confirmed by *ab initio* calculations (Kok *et al.* 1990) to be different, there should be unequal  $\Lambda$ -doublet population in the product, even though the initial  $\Lambda$ -doublets states are equally populated, as discussed earlier. Which  $\Lambda$ -doublet state,  $\Pi(A'')$  or  $\Pi(A')$ , is actually populated in the collision will depend on the relative signs of the average and difference potentials, as pointed out by Dagdigian *et al.* (1989).

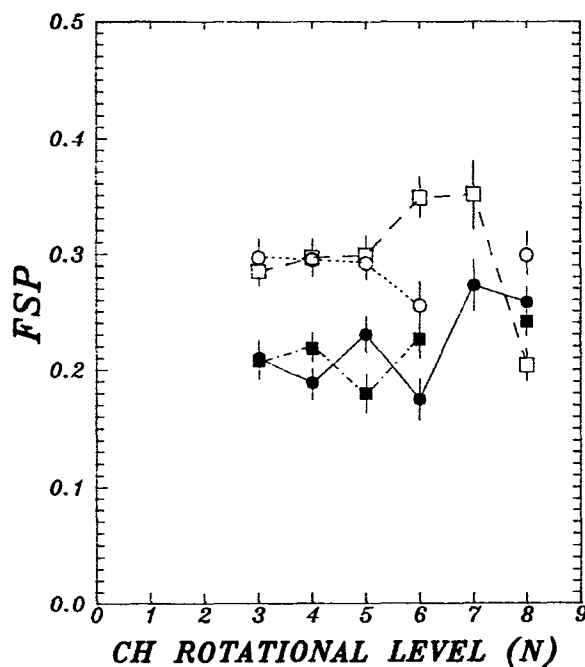
For the CH + He interactions, both the  $A'$  and  $A''$  PESs are generally repulsive as there is no possibility of reaction and the van der Waals region is very shallow. Thus the sum potential is generally positive. However, as mentioned above, the  $A''$  PES for CH + He has a radical orbital out of the CH–He plane, making it generally less repulsive everywhere relative to the  $A'$  PES where the orbital is in the plane. The average potential is mainly repulsive and hence has a positive sign, while the difference potential is predominantly negative. These circumstances lead to a preferential population of  $\Lambda$ -doublet states of  $\Pi(A'')$  symmetry, as observed experimentally. These experimental results for the unequal population of  $\Lambda$ -doublet states for CH + He are shown in figure 2, where the fine-structure probability (FSP) defined as the probability that a fine-structure state for a given  $N$  is populated taking the total probability for that  $N$  as one, is plotted as a function of  $N$ .

Also shown in the figure are the results for the FSP for the inelastic scattering of CH + D<sub>2</sub>. As is evident from figure 2, there is a preference for  $\Lambda$ -doublet states of  $\Pi(A'')$  symmetry in both collision systems. A comment is in order here. The theoretical description of inelastic scattering outlined in section 3.1 was formulated to treat a direct inelastic scattering process. For most angles of approach, CH + D<sub>2</sub> collision will be non-reactive with two PESs similar to those for CH + He. However, for the correct angle of approach, the  $A''$  PES develops a deep potential well corresponding to the electronic ground state of the methyl radical. Therefore, the rotationally excited CH radical produced in a collision between CH and D<sub>2</sub> can come from two distinct routes; direct inelastic scattering or complex formation and decomposition. By examining the isotope exchange channel in the same experiment (see section 4.2), it was found that the direct inelastic scattering route dominates. Furthermore, for the isotope exchange channel the FSPs of the isotopically distinct product exhibit oscillatory behaviour (Macdonald and Liu 1990b). It might be that the small oscillatory behaviour of the FSPs for inelastic scattering of CH with D<sub>2</sub> (see figure 1) is a residual of the complex formation/decomposition mechanism superimposed on the dominant preferential  $\Pi(A'')$  production from the direct inelastic scattering. However, as already mentioned, asymmetric  $\Lambda$ -doublet product state distributions arise from quantum interference between scattering amplitudes from the average and difference potentials. Hence, it would be expected that the asymmetry might be even greater for CH + D<sub>2</sub> than for CH + He, because in the former case the  $V_{A''}$  has a potential well and consequently the difference potential might be larger in magnitude resulting in stronger interference effects. But this is not in accord with the experimental observations, figure 2. Clearly, an extension of the theoretical treatment into a system with a chemical well will be warranted.





(a)



(b)

Figure 2. The fine-structure probability (FSP) is plotted for (a)  $\text{CH}(N=1) + \text{He} \rightarrow \text{CH}(N') + \text{He}$ , (b) the inelastic channel  $\text{CH}(N=1) + \text{D}_2 \rightarrow \text{CH}(N') + \text{D}_2$ .  $\circ$ ,  $\square$ :  $\Pi(A')$  symmetry; 1f, 2e respectively and  $\bullet$ ,  $\blacksquare$ :  $\Pi(A'')$  symmetry; 1e, 2f respectively. A preference for fine-structure states of  $\Pi(A'')$  symmetry is clearly evident. From Macdonald and Liu (1989, 1990a).

Another interesting observation about these inelastic scattering processes was the dependence on translational energy of the  $\Lambda$ -doublet preference. For a given  $\text{CH}(N)$  product level there are four energetically close fine-structure states; hence there are three independent fine-structure ratios. The only ratio, in both systems, that exhibited any dependence on translational energy was that involving  $\Lambda$ -doublet states of opposite symmetry, (i.e.  $\Pi(A'')/\Pi(A')$ ). As shown in figure 3, this ratio increased dramatically as the energetic threshold was approached. This phenomenon has also been seen in the recent detailed quantum close-coupling calculations of Wagner and Alexander (1990) on the  $\text{CH} + \text{He}$  system. Some speculation was made (Macdonald and Liu 1989) as to the cause of this effect but the exact origin needs further theoretical analysis.

For both systems, the experimental evidence suggests that at the rotational level of detail, that is summing over the fine-structure states with the same  $N$ , the collision dynamics is dominated by rotational rainbow scattering. Schinke (1981a, b) has shown that for inelastic scattering of closed-shell systems rotational rainbow features can also manifest themselves in state-resolved integral excitation function measurements. In other words, the energy dependence of the state-resolved integral cross-sections is in many respects reminiscent of the angular behaviour of the corresponding differential cross-sections when rainbow scattering dominates the dynamics. Two of these features are the observation of dynamical thresholds, and the existence of correlated rotational rainbow plots as shown in figure 4. Several interesting points are worth noting here. First of all, only the nearly mono-energetic molecular beams ( $\Delta E_0 \sim 0.1 \text{ kcal mol}^{-1}$ ) allowed us to observe the small dynamical thresholds,  $\Delta E_{\text{th}}$ . Secondly, in the case of  $\text{CH} + \text{He}$ , both criteria were used to identify the rotational rainbow features in the integral cross-section measurements. This is not a trivial point, the concept of rotational rainbow scattering has been applied only to closed-shell systems. For an open-shell system each rotational level is split into several fine-structure states; thus, it is not clear *a priori* how to extend the rotational rainbow concept to open-shell systems. Furthermore, the significance of the observation of rotational rainbows is to allow a direct connection of the anisotropy of the PES, as shown by equation (1). However, as mentioned earlier, the dynamics of the present systems are governed by two PESs, each with a different anisotropy. Presently it is not clear how the observed rotational rainbow features can be used to extract information about these two PESs. Further theoretical developments in this direction would be extremely useful and desirable. Finally, in the case of  $\text{CH} + \text{D}_2$ , the break in the product rotational level distribution occurred two units of angular momentum lower than that expected from the rotational rainbow correlation as illustrated by the dashed line in figure 4. To date, the theoretical work on rotational rainbow dynamics has only dealt with molecule + atom scattering. For the inelastic scattering between two rotors, the resulting rainbow correlation as illustrated in figure 4 may not be applicable. It is speculated that this 'unexpected' behaviour is a manifestation of multiple-impact rotational rainbow phenomenon. The reason for this is briefly as follows:  $\text{D}_2$ , being a homonuclear diatomic molecule, can only undergo even changes in  $\Delta J$  and hence the lowest energetic transition is to  $\text{D}_2 (J=2)$ . The classical rotational frequency of  $\text{CH} (N=4)$ , where the break in the state distribution occurs (see figure 3), and of  $\text{D}_2 (J=2)$  are almost identical. This, in combination with other observations (Macdonald and Liu 1990a), suggests that at the rotational level of detail the collision is governed by multiple-impact rotational rainbows, which in turn establishes a frequency-locking phenomenon between the receding rotors,  $\text{CH}$  and  $\text{D}_2$ .

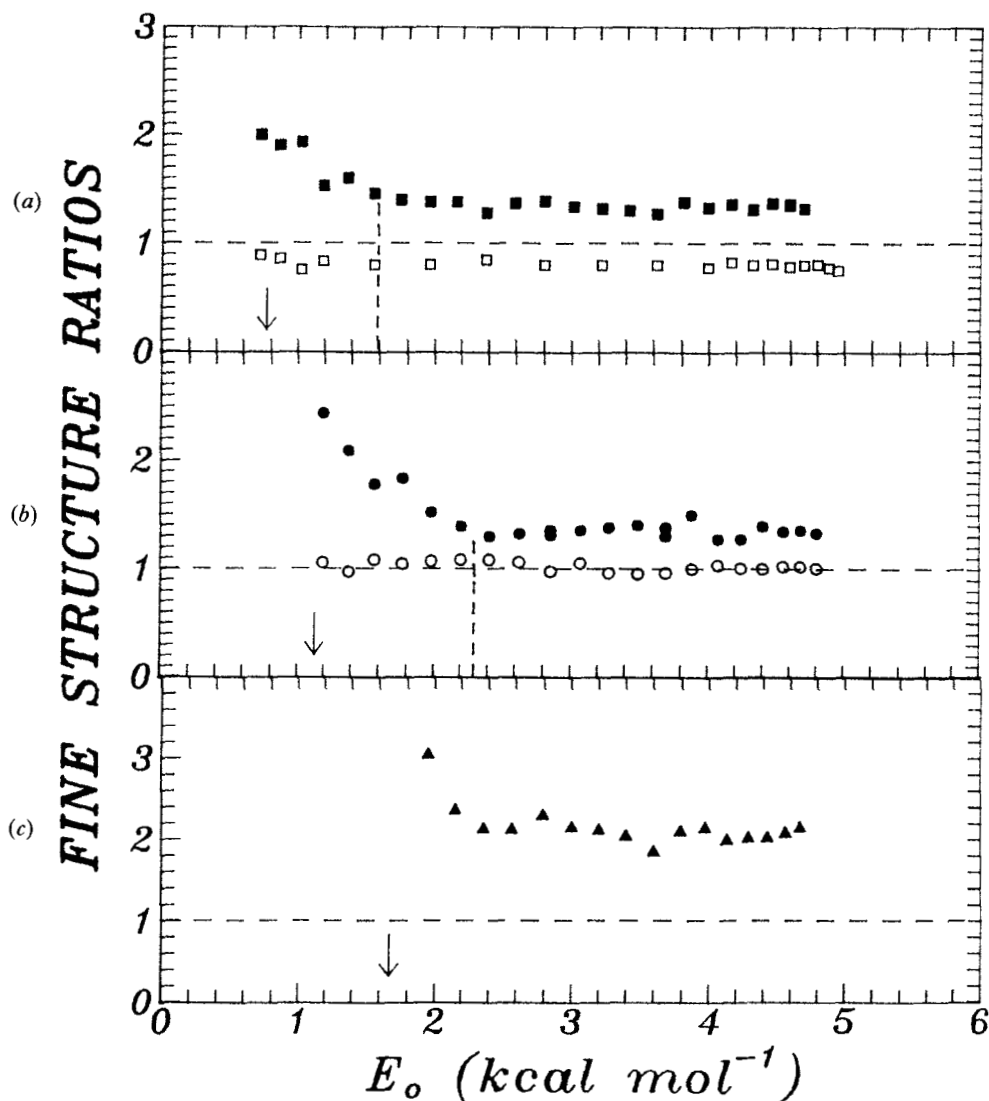


Figure 3. The collision energy dependence of the fine-structure ratios for the inelastic scattering of  $\text{CH}(N=1) + \text{D}_2 \rightarrow \text{CH}(N') + \text{D}_2$ . (a)  $N'=4$ ;  $\blacksquare$   $2e/2f$ ,  $\square$   $(1f/2e)g$ , (b)  $N'=5$ ;  $\bullet$   $1f/1e$ ,  $\circ$   $(1e/2f)g$  and (c)  $N'=6$ ;  $\blacktriangle$   $(2e/1e)g$ . The degeneracy of the  $F_1$  and  $F_2$  manifolds is accounted for by the factor  $g$  and statistical expectations are indicated by the horizontal dashed lines. From Macdonald and Liu (1990a).

As mentioned earlier, for the  $\text{CH} + \text{He}$  system there is now a close-coupling quantum calculation using accurate *ab initio* PESs (Kok *et al.* 1990). Preliminary comparisons between the theory (Wagner and Alexander 1990) and experiment are very encouraging. All the main features of the dynamics are in agreement but some subtle differences exist. Further efforts on both the electronic structure and close-coupling calculations are in progress to resolve these differences.

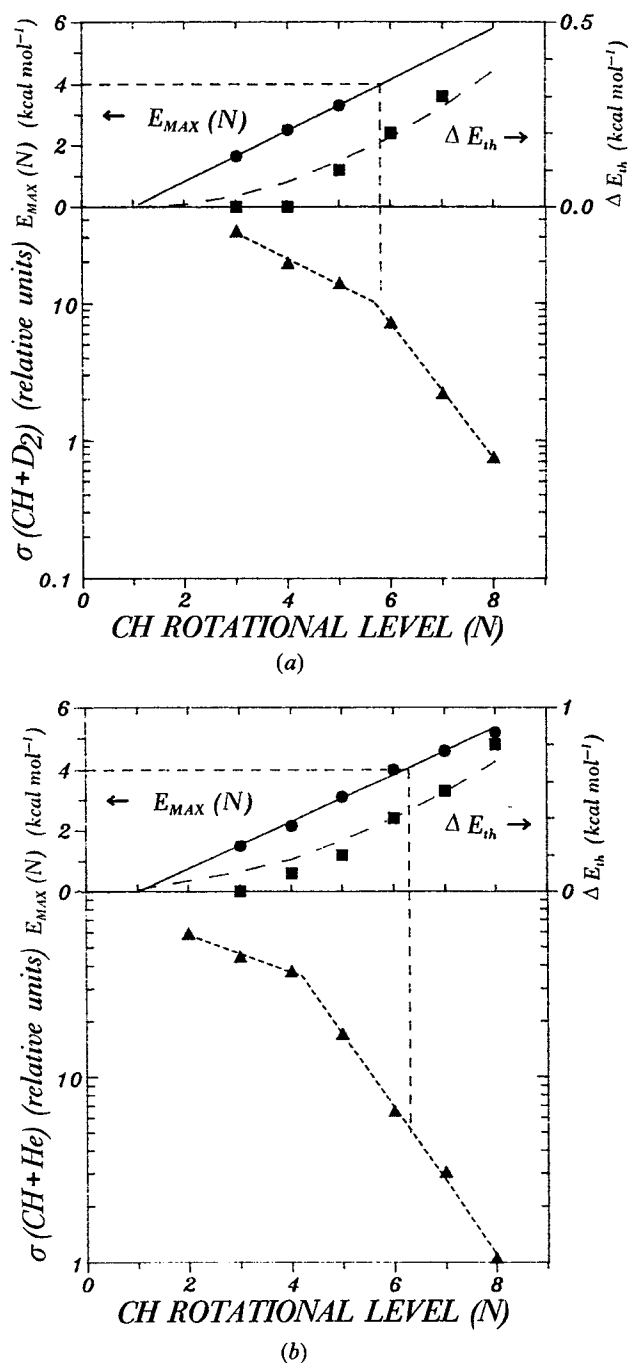


Figure 4. Rotational rainbow plot for the inelastic scattering of (a)  $\text{CH}(N=1) + \text{He} \rightarrow \text{CH}(N') + \text{He}$  and (b)  $\text{CH}(N=1) + \text{D}_2 \rightarrow \text{CH}(N') + \text{D}_2$  at  $E_0 = 4 \text{ kcal mol}^{-1}$ . The 'break' in the rotational level distribution is correlated with the maxima in the excitation functions, as indicated by the connected horizontal and vertical dashed lines. The rotational level dependence of dynamic threshold,  $\Delta E_{th}$ , is also shown in the top of each panel. The expected quadratic dependence on  $N$  is indicated by the long-dashed curves. From Macdonald and Liu (1989a, b).

### 3.2.2. OH( $X^2\Pi$ ) + H<sub>2</sub>( $^1\Sigma_g^+$ ) and N<sub>2</sub>( $^1\Sigma_g^+$ )

The inelastic scattering of OH + H<sub>2</sub> has been studied by Andresen *et al.* (1984) in a pioneering work. This was the first crossed-beam investigation of state-resolved rotational energy transfer of a transient radical. As described in section 2 the OH was prepared, almost exclusively in its lowest rotational level, in a supersonic expansion and single quantum states of the OH product were probed by LIF. For a comparison, some recent results on the inelastic scattering of OH + N<sub>2</sub> (Sonnenfroh *et al.* 1990) are also included. To the extent that the target molecule can be approximated as a structureless collision partner, which will be true for  $J=0$ , the basic concepts outlined in section 3.1 will be applicable.

In the collision energy range of the experiments, the  $V_{A'}$  and  $V_{A''}$  potential energy surfaces for both systems are characterized as predominantly repulsive (Kochanski and Flower 1981). Reactive channels are available but at higher energies than sampled. For either OH + H<sub>2</sub> or N<sub>2</sub>, both the A' and the A'' PESs involve OH electronic orbitals in and out of the plane of the reactants. For the A' PES, the OH radical orbital is in the plane while the doubly occupied orbital is out of the plane. For the A'' PES, the situation is reversed. In as much that one would expect a doubly occupied orbital to be a stronger centre of repulsive force than a radical orbital, the A' PES would be expected to be less repulsive than the A'' PES, resulting in a positive difference potential, opposite the case for CH.

The product state distributions for the inelastic scattering of OH( $X^2\Pi_{3/2}$ ,  $J=3/2$ ) + H<sub>2</sub> and N<sub>2</sub> at a collision energy of  $\sim 1.9$  kcal mol<sup>-1</sup> are shown in figures 5 and 6(a) respectively. As can be seen from the figure, both systems display a rapid decrease in rotational excitation within a spin-orbit manifold with increasing rotational quantum number. This is a general characteristic of state-resolved integral cross-sections for rotational energy transfer. The origin of this effect is the general notion that rotational energy transfer is better referred to as angular momentum transfer because not only must energy be transferred in the collision but also a torque must be applied to the rotor to cause rotational excitation. In passing we note that this is the very same reason for the occurrence of dynamical thresholds in rotational rainbow scattering, as discussed for CH + He. Perhaps more significant is the fact that the N<sub>2</sub> system shows a slightly faster decline in cross-section with increasing  $N$  than the H<sub>2</sub> system. Although the mass factors of the two collision systems are quite different, the dominant dynamical effect is believed to be the differences in the anisotropy of the PESs of the two systems. In a closely related study on the inelastic scattering of NO( $X^2\Pi_{1/2}$ ) + noble gas atoms, Joswig *et al.* (1986a) found that mass factors only played a minor role in determining the product rotational distribution. Furthermore, at a higher initial translational energy, as shown in figure 6(b) the product state distribution for OH + N<sub>2</sub> truncates at only half the available energy. This situation should be contrasted to the case of CH + He and D<sub>2</sub> where the rotational levels at the energetic limit were always found to be populated. As discussed earlier, the CH cases are dominated by rotational rainbow scattering and loosely speaking are classified as to the moderate to extreme coupling categories. In this sense the OH + N<sub>2</sub> scattering is better described as a weak coupling case. This classification is also in accord with an estimate of total inelastic cross-section for OH + N<sub>2</sub> (Sonnenfroh *et al.* 1990), which is an order of magnitude smaller than that for either OH + H<sub>2</sub> or CH + He.

Both systems indicate significant cross-sections for changes in spin-orbit manifold  $\Pi_{3/2} \rightarrow \Pi_{1/2}$  transitions. The OH radical is best described as an intermediate coupling case, though at low  $J$  the coupling scheme moves towards Hund's case (a). In either case

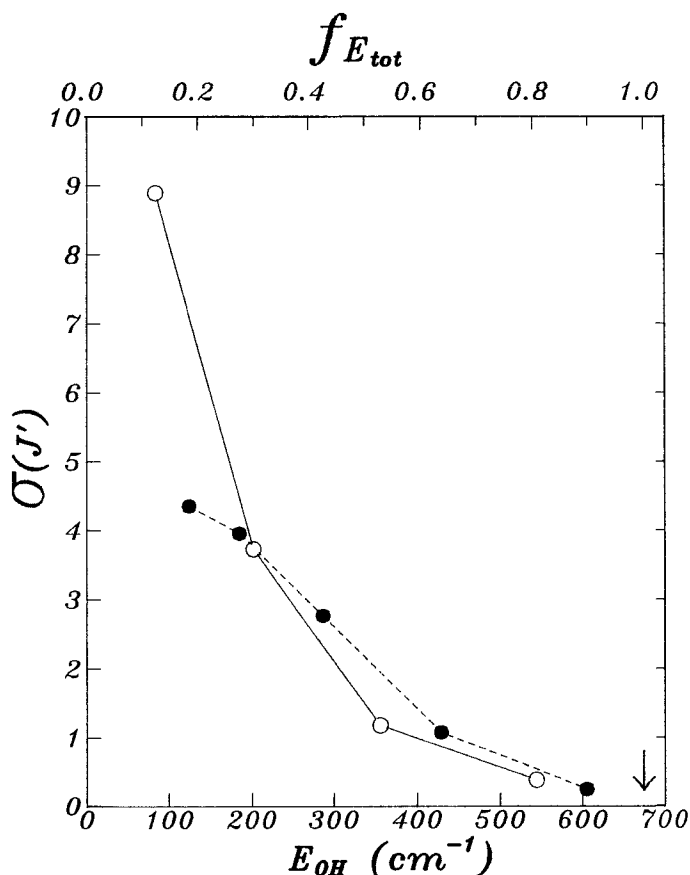


Figure 5. The relative cross-sections for the inelastic scattering of  $\text{OH} + \text{H}_2$  at  $E_0 = 1.92 \text{ kcal mol}^{-1}$   $\text{OH}(^2\Pi_{3/2}, J = \frac{3}{2}) + \text{H}_2 \rightarrow \text{OH}(^2\Pi_{3/2, 1/2}, J') + \text{H}_2$ . Only transitions with final fine-structure states of  $\Pi(A')$  symmetry are plotted;  $\circ$   $\Pi_{3/2}, e$  and  $\bullet$   $\Pi_{1/2}, f$ . At the top of the figure the internal OH energy is indicated as a fraction of the available energy,  $f E_{tot}$ . From Andresen *et al.* (1984).

the transitions between spin-orbit manifolds depends primarily on the magnitude of the difference potential. From figures 5 and 6, it is seen that spin-orbit changing transitions are larger with  $\text{H}_2$  as target than with  $\text{N}_2$ . This implies that in the two systems the difference potential is larger in the  $\text{OH} + \text{H}_2$  system. A more sensitive probe of the difference potential is the  $\Lambda$ -doublet state distribution at higher rotational quantum numbers. As already discussed, the  $\Lambda$ -doublet asymmetry results from an interference phenomenon from the average and difference potentials. Dagdigian *et al.* (1989) pointed out that for the OH radical, which has a  $\pi^3$  electron occupancy, the  $V_{A''}$  potential is expected to be more repulsive than the  $V_{A'}$  potential for the reasons discussed above. This implies that constructive interference will favour the production of  $\Lambda$ -doublet states with  $\Pi(A')$  symmetry. These expectations are borne out in the experimental measurements for both the  $\text{OH} + \text{H}_2$  (Andresen *et al.* 1984) and  $\text{OH} + \text{N}_2$  (Sonnenfroh *et al.* 1990) systems. The degree of preference is smaller in the latter case, for instance for the  $\text{OH}(\Pi_{3/2}, J = 11/2)$ ,  $\Pi(A'')/\Pi(A') \sim 4.5$  for the  $\text{OH} + \text{H}_2$  system and

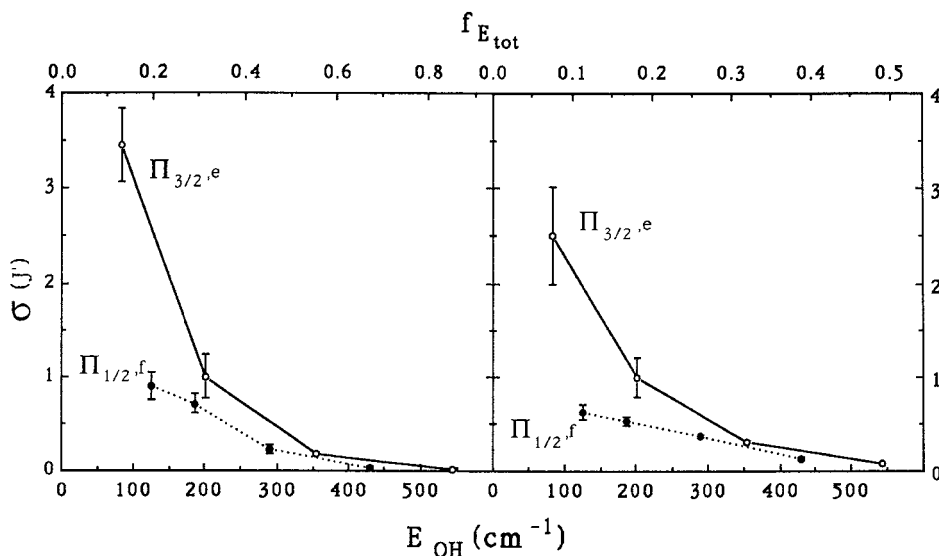


Figure 6.  $\text{OH}(X^2\Pi_{3/2}, J=\frac{3}{2}) + \text{N}_2 \rightarrow \text{OH}(X^2\Pi_{3/2, 1/2}, J, e/f) + \text{N}_2$ . The relative cross-sections for the inelastic scattering of  $\text{OH} + \text{N}_2$  for two translational energies (a)  $E_0 = 1.83 \text{ kcal mol}^{-1}$ , (b)  $E_0 = 3.18 \text{ kcal mol}^{-1}$ . Only final states of  $\Pi(A)$  symmetry are shown. The  $f_{E_{\text{tot}}}$  is indicated at the top of each panel. From Sonnenfroh *et al.* (1990).

approximately 1.8 for the  $\text{OH} + \text{N}_2$ . This again implies that the difference potential in the  $\text{OH} + \text{N}_2$  system is smaller than that in the  $\text{OH} + \text{H}_2$  system.

Because inelastic scattering in the  $\text{OH} + \text{H}_2$  system has important astrophysical implications (Andresen 1986), there are several detailed theoretical calculations on this system (Schinke and Andresen 1984, Dewangan *et al.* 1986, 1987) fitting potential energy surfaces to *ab initio* potential energy results by Kochanski and Flower (1981). The first two of these studies report close-coupling and the third coupled-states calculations. It should be noted that all the calculations were done for  $\text{H}_2$  ( $J=0$ ), whereas in the experiments at least 75% of the  $\text{H}_2$  have  $J \geq 1$  because of nuclear spin statistics. In general there was good overall agreement with the experimental measurements of Andresen *et al.* (1984), except for reproducing the  $\Lambda$ -doublet propensity which was calculated to be too large. Dewangan *et al.* (1986) were able to get better agreement for the observed  $\Lambda$ -doublet propensity in the  $F_1$  manifold but not the  $F_2$  manifold using a  $V_{22}$  coupling matrix element a factor of two smaller than that found in the *ab initio* calculations. This illustrates how sensitive these propensities are to the fine details of the potential energy surfaces.

Both inelastic scattering systems are directly related to important combustion reactions,  $\text{H} + \text{H}_2\text{O} \rightarrow \text{OH} + \text{H}_2$  and  $\text{H} + \text{N}_2\text{O} \rightarrow \text{OH} + \text{N}_2$ . Both of these chemical reactions have been studied by a combination of the hot-atom and LIF techniques. In these investigations the OH product  $\Lambda$ -doublet state distributions were found to be statistical for the  $\text{H} + \text{H}_2\text{O}$  reaction (Kleinermans *et al.* 1989) and to have a  $\Pi(A') > \Pi(A'')$  propensity for  $\text{H} + \text{N}_2\text{O}$  (Hollingsworth *et al.* 1985). Although the initial conditions for the reactive and inelastic scattering events are different, conceptually the exit channel interactions of a reactive encounter can be regarded as a half inelastic scattering event. Because of this intimate connection between reactive and inelastic scattering, it is interesting to ask to what extent the observed  $\Lambda$ -doublet selectivity in a

chemical reaction can be traced to exit-channel inelastic effects. We will return to this point in section 4.

### 3.2.3. $\text{NH}(\text{X}^3\Sigma^-) + \text{Ar}(^1\text{S})$ and $\text{NH}(\text{a}^1\Delta) + \text{Ar}(^1\text{S})$

An interesting example of some of the physical concepts for the inelastic scattering of open-shell species presented in section 3.1 is provided by rotational energy transfer of the NH radical in the ground and metastable electronic states,  $\text{NH}(\text{X}^3\Sigma^-) + \text{Ar}$  (Dagdikian 1989) and  $\text{NH}(\text{a}^1\Delta) + \text{Ar}$  (Sauder *et al.* 1989). In both experiments the crossed-beam and LIF techniques were employed to obtain the radical product state distribution.

For collisions of  $^{2S+1}\Sigma$  radicals and spherically symmetric collision partners there is only a single PES involved. The  $\text{NH}(\text{X}^3\Sigma^-)$  radical is well described by Hund's case (b) coupling so that the three fine-structure states are well characterized by states of definite parity labelling. As noted in section 3.1, in general, the scattering cross-section for  $^{2S+1}\Sigma$  radicals cannot be separated into a spin-dependent geometric factor and a purely dynamical factor. However, Dagdikian (1989) showed that a completely general scaling relationship still exists which can be used to predict the relative cross-sections into the three spin states for a given  $N=0 \rightarrow N'$  transition. The experimentally observed ratio  $F_2/F_1$  and  $F_3/F_1$  as a function of  $N$  was in agreement with the predicted theoretical result and provides strong evidence for the validity of the theoretical description of the collision dynamics for  $^3\Sigma$  radicals.

Further evidence comes from an analysis of the inelastic collisions of the metastable  $\text{NH}(\text{a}^1\Delta)$  molecule and Ar (Sauder *et al.* 1989). Similar to inelastic collisions involving  $^{2S+1}\Pi$  molecules, there are two potential energy surfaces,  $V_{A''}$  and  $V_{A'}$ , governing the collision dynamics of  $^1\Delta$  molecules with spherically symmetric collision partners. However, unlike the case of a  $^2\Pi$  molecule, Sauder *et al.* (1989) showed that for  $\text{NH}(\text{a}^1\Delta)$  with a  $\pi^2$  electron occupancy, there is no simple prediction as to which potential energy surface,  $V_{A''}$  or  $V_{A'}$ , will be more or less repulsive because the dominant electronic configuration,  $\pi^2$ , has equal in-plane and out-of-plane character. This implies that the difference potential,  $\frac{1}{2}(V_{A''} - V_{A'})$ , may be small and the IOS scaling relationships for a  $^1\Delta$  state take on a simple form very similar to the case of rotational energy transfer in a  $^1\Sigma$  molecule. In fact, Sauder *et al.* (1989) argued that because the nominal electronic configuration of  $\text{NH}(\text{X}^3\Sigma^-)$  is also  $\pi^2$ , both  $\text{a}^1\Delta$  and  $\text{X}^3\Sigma^-$  states have equal mixtures of in-plane and out-of-plane  $\pi$  electron character, the interaction potential for  $\text{NH}(\text{X}^3\Sigma^-) + \text{Ar}$  will be similar to the average potential for  $\text{NH}(\text{a}^1\Delta) + \text{Ar}$ . Under sudden conditions, the base cross-sections for these two scattering systems are identical; thus the cross-sections for  $\text{NH}(\text{a}^1\Delta) + \text{Ar}$  can be predicted from the  $\text{NH}(\text{X}^3\Sigma^-) + \text{Ar}$  base cross-section measurements and angular momenta coupling coefficients. It is encouraging that the predicted value agrees rather well with the experiment although only one data point was available.

## 4. Reactive scattering

### 4.1. Some basic concepts

As far as the PES is concerned, two distinct features often characterize a chemical reaction involving radicals. First, because the radical contains unpaired electrons, multiple PESs are necessary to describe its collisional behaviour. The second common feature, almost universally true for a radical-radical collision system, but which may or may not be so for a radical-molecule system, is that the lowest PES usually has a potential well in going from reactants to products. As anticipated, the presence of these



features plays a significant role in the dynamics of radical reactions. To make a clear connection with the concepts developed for a single PES system, it is perhaps instructive to factor out the fine-structure effects from the rovibrational level distributions by summing up all the fine-structure populations associated with a given rovibrational quantum number for a given radical and analyse the results accordingly.

#### 4.1.1. Rovibrational level distributions

For a reaction system involving a potential well conventional wisdom suggests that the reaction will proceed through an intermediate complex and the product internal state distribution will then be governed by the statistical decomposition of the complex. Moreover, any significant deviation from the statistical distribution is often taken as a signature for the existence of a short-lived complex or some kind of dynamical bottleneck or exit channel effects. Clearly, the proper interpretation depends on the individual case. Here we merely want to focus on the statistical distribution, which is generic and has been discussed in the past in a different context (Davis 1985, Wittig *et al.* 1985). Nevertheless, we feel that it has particular significance in treating the radical reaction system.

All statistical theories of chemical reactions are based on two main assumptions: (1) there is a dividing surface that separates the intermediate complex from all dissociation products and the probability of complex formation or dissociation is only the probability of crossing that dividing surface in the correct direction, (2) at the dividing surface all configurations of the system that are consistent with the total energy and total angular momentum have equal probabilities of crossing the dividing surface. The first approximation assumes that a dividing surface that separates the complex and products (or reactants) can be found that is *clean*; that is the system does not change its direction along a reaction coordinate and re-cross the dividing surface. The second approximation assumes that the complex forgets its initial conditions and randomly explores phase space until it discovers the way out through the dividing surface. In order to calculate the final state distribution, one need only calculate the phase space available at the dividing surface for each observed product state at the asymptote. Statistical theories are generally similar in employing an adiabatic approximation whereby quantum numbers at the dividing surface can be correlated in a one-to-one fashion to quantum numbers at the asymptote. This leads to a direct calculation of product distributions. (Other types of statistical theories which take explicit account of exit channel effects are possible (Wagner and Parks 1976, Clary 1984, Light and Altenberger-Siczek 1976).) Statistical theories are different in the manner in which they define the dividing surface and compute the phase space available at that surface.

In general, statistical theories might be broadly classified as having 'tight' or 'loose' dividing surfaces. Variational transition state theory and RRKM theory (Truhlar *et al.* 1983) assume that the dividing surface encompasses degrees of freedom that are either internal vibrations or external overall rotations of the complex. This is a 'tight' dividing surface in that the free rotation and orbital motion of the reactants at the asymptote are assumed to have been rearranged into relatively tightly bound bending vibrations or overall rotations. While one can correlate a stretching vibration from dividing surface to reactant, a bending vibration at the dividing surface cannot be equated simply with a rotational state at the asymptote. Thus tight theories cannot usually be used to provide resolved product rotational distributions. A 'loose' statistical theory would be the phase space theory (PST) (Light 1967, Pechukas *et al.* 1966) in which the dividing surface encompasses the unchanged vibrational, rotational and orbital motion of the

reactants at the asymptote. Only the energy has changed, due to long-range forces, in going from reactants to dividing surface. Such a theory is only consistent with a PES that is dominated by spherically symmetric long-range forces because any substantial anisotropy would ultimately force the conversion of free rotations into bending vibrations. However, such theories do allow explicit calculation of rotationally resolved product distributions.

There are several statistical theories that do, in principle, allow a correlation of states at the dividing surface to rotational states of the products at the asymptote in the presence of substantially anisotropic components to the PES. Adiabatic channel theory (Quack and Troe 1974, Quack 1979) provides interpolative prescriptions for connecting quantum numbers along the reaction path. While successful for thermal rate constant determinations, this theory does not provide a prescription for calculating a correlation directly from a given PES and has not been used to generate rotational distributions for comparison to experiment. Recently Clary (1984, 1987) has developed a complex formation theory based upon a rotationally adiabatic capture approach. The rotational states along the reaction path are calculated on any given PES within the context of the body-fixed coordinate frame and its associated kinetic energy operator under the dynamical assumption that the projection of the total angular momentum on the body-fixed axis is a conserved quantity. This formulation allows a feasible calculation of rotationally adiabatic states that already incorporate much of the rotational-orbital interactions in the space-fixed frame at the price of ignoring certain relatively weak Coriolis couplings that make the projection of the total angular momenta constant in the space-fixed, and not the body-fixed, frame. Excellent agreement between calculations of his theory (Clary and Henshaw 1989) and experimental thermal rate constant measurements have been obtained for many exothermic radical reactions which proceed without a potential energy barrier. To date this formalism has not been applied to the product state distributions but extensions of the theory to do this are underway (A. Wagner 1989, work in progress). Qualitatively, the effects of the adiabatic capture approach on the product state distributions can be appreciated as follows.

Consider the isotope exchange reaction of  $\text{CH} + \text{D}_2 \rightarrow \text{CD} + \text{HD}$ . As CH approaches  $\text{D}_2$ , the long range dipole-quadrupole interaction will exert a torque on the molecules and leads to a preference for a collinear configuration, while at the same time the bending vibration frequency of the system about this preferred configuration will also increase. Further along the reaction path, a parallel arrangement of bonds occurs in which both in- and out-of-plane bending vibrational frequencies are relatively high (Dunning *et al.* 1986, Aoyagi *et al.* 1990). Deeper into the well, a final rearrangement occurs into the symmetric  $\text{CH}_3$  form with its quite large in-plane and relatively weak out-of-plane bending frequencies. The angular variation of this reaction path illustrates the importance of anisotropy in the  $A''$  PES. There should be different centrifugally corrected adiabatic barriers for different bending vibrational states (or hindered rotor states) and these in turn will be correlated with different asymptotic rotational states of the reactants. For this reaction the entrance ( $\text{CH} + \text{D}_2$ ) and exit ( $\text{CD} + \text{HD}$ ) channels are governed by the same interactions; thus, the same considerations for complex formation apply to complex decomposition as well. The net result is that the product state distributions could be different from those predicted by a PST treatment. In particular, this would be true for low translational energies for which adiabatic behaviour might be a better description than a sudden approximation.

It is interesting to note that the rotationally adiabatic capture picture just described has significant implications to oriented molecule scattering experiments (Bernstein

*et al.* 1987). A central question in stereospecific dynamics is the dependence of reactivity on the orientation of the reagents. For a chemical reaction with an activation barrier a key factor is the angle dependence of the potential barrier to reaction, whereas for a reaction with negligible barrier the orientation dependence of the centrifugal barrier needs to be considered. In either case, the reactivity is governed by the distribution of the attack angle at the barrier. If the long-range interaction potential is anisotropic enough, then as the reactants approach each other the asymptotically prepared oriented reactants will tend to re-orient themselves to the most favourable configuration leading to reaction. As a result, the distribution of the attack angle at the barrier need not mirror the asymptotic distribution. Intuitively, this re-orientation effect is expected to be more pronounced at low collision energies, that is the adiabatic limit. Whether it tends to enhance or diminish the anticipated reactive asymmetry in an oriented molecule scattering experiment will depend on the individual case. In any event, it should be clear that measuring the steric effects as a function of the collision energy will provide the most direct means of obtaining the angle dependence of the barrier to reaction and allow further insights into the stereospecific dynamics.

#### 4.1.2. Fine-structure effects

There are now many examples of preferential product fine-structure state distributions in both reactive and photodissociative processes, as illustrated in table 3. In the case of spin–multiplet selectivity from the photodissociative production of a  $^{2S+1}\Sigma$  fragment, various interpretations have emerged. For example, in the  $\text{SO}_2$  case, a mechanism based on a singlet–triplet crossing, induced by the spin–orbit coupling, in the exit channel was proposed (Kanamori *et al.* 1985). In the case of the ICN photodissociation, a model (Joswig *et al.* 1986b) was given in terms of out-of-plane, spin-dependent forces resulting from the coupling of the total angular momentum of the receding I atom with the rotational angular momentum of the CN fragment. Finally a symmetry argument was invoked to rationalize the results for IR multiphoton dissociation of  $\text{HN}_3$  (Alexander *et al.* 1988b), in the same fashion as that for  $\Lambda$ -doublet selectivity (discussed below) but extended to include the spin coordinates.

In almost every case the  $\Lambda$ -doublet selectivity, notably for  $^2\Pi$  radicals, has been interpreted in terms of an electronic symmetry argument by analysis of the evolution of the molecular orbitals of the precursor which adiabatically correlate with the unfilled  $\Pi$  orbital in the radical product. One notable exception is the state-to-state photodissociation dynamics of the  $\text{H}_2\text{O}$  molecule studied by Hausler *et al.* (1987), in which this simple interpretation broke down completely. To account for the observed oscillatory behaviour in the fine-structure state distributions of the photofragment OH, it was necessary to invoke a full quantum mechanical theory specifically formulated for the process being studied.

In our opinion, the  $\Lambda$ -doublet selectivity may be altogether much more complicated than the simple symmetry argument suggests. First, if this simple picture were correct, then it should be able to qualitatively rationalize the state-to-state photodissociation experiment on the  $\text{H}_2\text{O}$  molecule. Secondly, as discussed in section 3.1, the inelastic scattering of non- $\Sigma$  state radicals is governed by multiple PESs, whereas the simple picture completely ignores the nature of the multiple PES despite the fact that at long range the description of the interactions between the receding fragments must involve multiple PESs just as in the case of inelastic scattering. In the following we will first present our view about  $\Lambda$ -doublet selectivity, which makes a close connection among the reactive, photodissociative and inelastic processes, then some comments regarding the simple picture will be given.

Table 3. Examples of preferential fine-structure distribution in reactive and photodissociative processes.

System	Selectivity	References
<i>Reaction</i>		
H + NO <sub>2</sub> → OH( <sup>2</sup> Π) + NO → OH + NO( <sup>2</sup> Π)	Π(A') > Π(A''); F <sub>1</sub> ≈ F <sub>2</sub> Π(A') > Π(A''); F <sub>1</sub> > F <sub>2</sub>	Mariella and Luntz (1977) Sauder and Dagdigian (1990)
O( <sup>1</sup> D) + H <sub>2</sub> → OH( <sup>2</sup> Π) + H	Π(A') > Π(A'')	Butler <i>et al.</i> (1986)
H + N <sub>2</sub> O → OH( <sup>2</sup> Π) + N <sub>2</sub>	Π(A') > Π(A'')	Hollingsworth <i>et al.</i> (1985)
H + O <sub>2</sub> → OH( <sup>2</sup> Π) + O	Π(A') > Π(A'')	Kleinermanns <i>et al.</i> (1989) Bronikowski <i>et al.</i> (1989)
CH(N = 1) + D <sub>2</sub> → CD( <sup>2</sup> Π) + HD	Oscillatory	Macdonald and Liu (1990b)
<i>Photodissociation</i>		
SO <sub>2</sub> $\xrightarrow{193\text{ nm}}$ SO( <sup>3</sup> Σ <sup>-</sup> ) + O	F <sub>1</sub> , F <sub>3</sub> > F <sub>2</sub>	Kanamori <i>et al.</i> (1985)
ICN $\xrightarrow{>249\text{ nm}}$ CN( <sup>2</sup> Σ) + I	Oscillatory	Joswig <i>et al.</i> (1986b)
HN <sub>3</sub> $\xrightarrow{\text{n.i.r.}}$ NH( <sup>3</sup> Σ <sup>-</sup> ) + N <sub>2</sub> NH*( <sup>1</sup> Δ) + N <sub>2</sub>	F <sub>1</sub> , F <sub>3</sub> > F <sub>2</sub> Δ(A') > Δ(A''); <b>V</b>    <b>J</b>	Stephenson <i>et al.</i> (1988) Stephenson <i>et al.</i> (1988)
H <sub>2</sub> O $\xrightarrow{\text{i.r.}}$ H <sub>2</sub> O(V, J, K) $\xrightarrow{193\text{ nm}}$ OH( <sup>2</sup> Π) + H	Oscillatory	Hausler <i>et al.</i> (1987)
NO <sub>2</sub> $\xrightarrow{488\text{ nm}}$ NO <sub>2</sub> * $\xrightarrow{488\text{ nm}}$ NO( <sup>2</sup> Π) + O( <sup>1</sup> D)	Oscillatory	Bigio and Grant (1985)
NH <sub>3</sub> $\xrightarrow{<135\text{ nm}}$ NH*( <sup>1</sup> Π) + H <sub>2</sub>	Π(A') > Π(A'')	Quinton and Simons (1981)
HONO $\xrightarrow{355\text{ nm}}$ OH( <sup>2</sup> Π) + NO $\xrightarrow{355\text{ nm}}$ OH + NO( <sup>2</sup> Π)	Π(A') > Π(A''); F <sub>2</sub> > F <sub>1</sub> Π(A') > Π(A''); F <sub>2</sub> > F <sub>1</sub>	Vasudev <i>et al.</i> (1984) Dixon and Rieley (1989)
H <sub>2</sub> O <sub>2</sub> $\xrightarrow{>248\text{ nm}}$ OH( <sup>2</sup> Π) + NO <sub>2</sub>	Π(A') > Π(A''); <b>V</b>    <b>J</b>	Gericke <i>et al.</i> (1986) Docker <i>et al.</i> (1988)
HNO <sub>3</sub> $\xrightarrow{280\text{ nm}}$ OH( <sup>2</sup> Π) + NO <sub>2</sub>	Π(A') > Π(A''); <b>V</b>    <b>J</b>	August <i>et al.</i> (1988)
CH <sub>3</sub> ONO $\xrightarrow{364\text{ nm}}$ NO( <sup>2</sup> Π) + CH <sub>3</sub> O	Π(A') > Π(A'')	Bruhmann and Huber (1987, 1988)
NOCl $\xrightarrow{>450\text{ nm}}$ NO( <sup>2</sup> Π) + Cl	Π(A') > Π(A''); <b>V</b>    <b>J</b> F <sub>2</sub> > F <sub>1</sub>	Lahmani <i>et al.</i> (1986) Ticktin <i>et al.</i> (1988)
HCOOH $\xrightarrow{225\text{ nm}}$ OH( <sup>2</sup> Π) + HCO	Π(A') ~ Π(A''); <b>V</b>    <b>J</b> F <sub>2</sub> ≤ F <sub>1</sub>	Brouard and O'Mahony (1988)

From the spectroscopic viewpoint the origin of the Λ-doubling can be described as follows (Herzberg 1950). In a non-rotating diatomic molecule the electron orbital angular momentum (**L**) precesses rapidly about the internuclear axis with a quantized projection of *Λ* as a result of the axial symmetry of the electrostatic field from the nuclear charges. As the molecule rotates, Λ-doublet splitting occurs as a consequence of breaking the axial symmetry by the nuclear rotation–electron orbital angular momentum coupling. This can be regarded as the beginning of the L-uncoupling phenomenon, an intrinsically non-adiabatic behaviour.

Now let us consider a scattering process such as the isotope-exchange reactions of CH + D<sub>2</sub> → CD + HD for illustration. As D<sub>2</sub> approaches CH, the axial symmetry of the charge distribution of CH is lifted because of the intermolecular interaction. The 'goodness' of the quantum number *Λ* deteriorates as the identity of the reactive intermediate evolves and will eventually be destroyed when the CHD<sub>2</sub>\* activated complex has fully developed. Conceptually, this process is very similar to the L-uncoupling phenomenon just described, except that in the present case the uncoupling

of the electron orbital angular momentum from the CH internuclear axis is dictated by intermolecular interactions, rather than rotational coupling in the isolated CH radical. When the  $\text{CHD}_2^*$  complex decomposes, this chemically mediated L-uncoupling process simply occurs in reverse; there is an L-recoupling of the electron orbital angular momentum to the CD product internuclear axis. Conceivably, this L-recoupling process occurs in a relatively localized region on the PES where the old bonds have dissolved and the new ones have just been born. This implies that much of the product fine-structure selectivity could result from the L-recoupling mechanism which normally involves extensive electronic reorganization as the nuclear motions evolve, because the fine-structure state can be regarded as a direct consequence of the coupling between electronic and nuclear motions. In other words, the product fine-structure selectivity can be regarded as a realignment of the electron angular momenta in the body-fixed frame to or from the molecular frame. This realignment may be correlated with the electronic charge redistribution. Upon further separation between the product fragments, this 'nascent' fine-structure distribution could be moderated by inelastic scattering processes due to the interaction between the receding fragments. As a result, the final fine-structure state distribution is the net outcome of the interplay between the 'selectivity' originating from the transition state region and the 'modification' of this distribution by the subsequent inelastic collision.

Another effect closely related to the L-uncoupling phenomenon is the spin-orbit (S-O) interaction, which is absent in the reaction intermediate  $\text{CH}_3(\tilde{X}^2A'')$ . But both the reagent  $\text{CH}(X^2\Pi)$  and product  $\text{CD}(X^2\Pi)$  radicals possess non-zero S-O constants, so that as the reaction proceeds the S-O interaction will first be quenched on forming  $\text{CHD}_2^*$  and then increase again as the complex fragments. This diminishment and growth of the S-O interaction is, of course, occurring concurrently with L-uncoupling and L-recoupling. Thus, spin may participate in the chemical reaction in a more active manner. This should be contrasted to the direct inelastic scattering process in which the spin can be treated as a spectator, see section 3.1.

The concept that a reactive event can be envisaged to proceed through two, more or less, distinct interaction regions and that the product fine-structure state distribution is determined from the corresponding transition probability amplitudes, has a strong similarity to that for the photodissociation process, as exemplified by the state-to-state studies on the  $\text{H}_2\text{O}$  molecule (Andresen and Schinke 1988). This can be appreciated readily if one considers the transition state region and the subsequent inelastic collision in reactive scattering to be similar to the Franck-Condon region and the final state interaction in photodissociation process respectively. However, unlike the photodissociation case, even a perfect state-to-state reactive scattering experiment will still involve substantial averaging over the initial conditions such as impact parameter (or orbital angular momentum) and orientation, which as well as smoothing from the exit channel inelastic collisions, would undoubtedly reduce the 'selectivity' originating from the transition state region. Nevertheless, the dominant dynamical features would survive this averaging in many reaction systems.

From this viewpoint let us now examine the simple picture just discussed. In this model an assumption is made of a coplanar process, that is the plane of rotation of the radical fragment is the same as the plane of the precursor or complex throughout the process; thus the preferential production of a given  $\Lambda$ -doublet component reflects the conservation of electronic wavefunction symmetry with respect to this plane. Because the assumption of a coplanar process is rarely justified or confirmed by other experimental evidences (e.g. fragment ( $\mathbf{v}$ ,  $\mathbf{J}$ ) correlations), care must be exercised in applying this model, which is in essence an electronically adiabatic model, to interpret

the fine-structure selectivity. Any non-planar motions during the break-up of the complex will induce dynamic couplings between the adiabatic  $V_{A'}$  and  $V_{A''}$  PESs. Another way of viewing this as follows. The adiabatic PESs  $V_{A'}$  and  $V_{A''}$ , are defined in the body-fixed (i.e. collision) frame, whereas the electronic wavefunction reflection symmetries of the  $\Lambda$ -doublet components,  $\Lambda(A')$  and  $\Lambda(A'')$ , are defined with respect to the plane of rotation of product molecular frame and in the high  $J$  limit (Alexander and Dagdigan 1984). Only for a strictly coplanar process and in the high  $J$  limit, could there be a one-to-one correspondence between the  $\Lambda$ -doublet state of  $\Lambda(A')$  ( $\Lambda(A'')$ ) symmetry and the PES of  $V_{A'}$  ( $V_{A''}$ ). Otherwise a frame transformation will be required in treating the dynamics, which inevitably couples the two adiabatic PESs as illustrated for the inelastic scattering (section 3.1).

## 4.2. Specific systems

### 4.2.1. $H + NO_2 \rightarrow OH + NO$

This is one of the most studied atom-radical reactions. It is fast and exothermic, with a heat of reaction of  $-29 \text{ kcal mol}^{-1}$ . The approach of  $H(^2S)$  to  $NO_2(\tilde{X}^2A_1)$  yields two PESs, which in  $C_s$  symmetry can be classified as  $^1A'$  and  $^3A'$ . The reaction is thought to proceed along the singlet surface leading to the formation of a reactive intermediate of highly internally excited nitrous acid  $HONO^*(\tilde{X}^1A')$ . The triplet surface possesses a high barrier and plays only a small role in the reaction. On the exit channel side, there are a total of eight surfaces which asymptotically correlate to  $OH(X^2\Pi)$  and  $NO(X^2\Pi)$  products, with two surfaces each for  $^1A'$ ,  $^1A''$ ,  $^3A'$ ,  $^3A''$  in  $C_s$  symmetry.

Dynamically, this reaction has been the testing ground for various experimental techniques. The translational energy disposal was found to be about 25% of the reaction exoergicity by two different methods in crossed-beam experiments (Haberland *et al.* 1974 and 1980, Murphy *et al.* 1981). The vibrational state distribution of the OH product has been measured by i.r. chemiluminescence (Wichramaaratchi *et al.* 1984, Klenerman and Smith 1987), ESR (Spencer and Glass 1976) and LIF (Silver *et al.* 1976, Mariella *et al.* 1978) techniques. The distributions were found to fall monotonically with increasing  $v$  and accounted for 25% of the available energy. The OH rotational distribution has been characterized by the LIF technique in two crossed-beam experiments and accounted for 22% of the total energy. From these measurements, it is expected that 28% of the exoergicity should appear as internal NO excitation. Very recently, Sauder and Dagdigan (1990) report a crossed-beam study to characterize the internal state distribution of NO product from this reaction using the LIF technique. They found that only 6% and 4% of the available energy appeared in NO rotational and vibrational excitations respectively. Similar, but not quite identical, results have been obtained by Smith and co-workers (Irvine *et al.* 1989). They found that 10% and 5.6% of the available energy appeared in NO rotational and vibrational excitations respectively. This is considerably less than the 28% internal energy disposal predicted for NO from the energy balance considerations of the previous results. It appears that despite the numerous experimental efforts over the past 15 years, there are still some uncertainties which remain for this reaction.

Mechanistically, the presence of the deep HONO potential well on the  $^1A'$  PES suggests an addition-elimination reaction mechanism. The observed nearly isotropic but slight-forward peaking angular distribution (Haberland *et al.* 1974, 1980, Murphy *et al.* 1981) support this mechanism and indicate the intermediate lifetime to be of the order of one rotational period or less. A simple PST calculation (Sauder and Dagdigan

1990), with a loose transition state approximation, neglecting fine-structure effects, reveals that both the observed OH rotational and vibrational state distributions are considerably hotter than those predicted by PST, whereas the observed internal NO excitations have significantly less energy than those expected from statistical consideration. This comparison is roughly in accord with the existence of a short-lived complex, because the result of more energy disposed in the new bond (OH) than in the old bond (NO) is generally the expectation for a more direct reaction of the  $A + BCD \rightarrow AB + CD$  type. However, in view of the problem of energy balance, it still remains to be seen how well this conclusion will hold.

Both reaction products, OH and NO, are  $^2\Pi$  radicals; hence their  $\Lambda$ -doublet and spin-orbit populations are of considerable interest. As indicated in table 3, the  $\Lambda$ -doublet states with  $\Pi(A')$  symmetry are preferentially populated for both OH and NO. These propensities were interpreted, in both cases (Mariella and Luntz 1977, Sauder and Dagdigian 1990), in terms of the adiabatic orbital correlation model, as outlined in section 4.1. We neither want to criticize the validity of that model in this particular reaction, nor support it here, despite the fact that it seems possible to rationalize the observations for both products in a qualitative sense. We merely want to point out our concerns based on two other experimental observations.

First, an approximately equal spin-orbit population was observed for the OH product (Mariella *et al.* 1978, Murphy *et al.* 1981), while  $F_1$  ( $\Omega = \frac{1}{2}$ ) was found to be preferentially populated over  $F_2$  ( $\Omega = \frac{3}{2}$ ) for the NO product (Sauder and Dagdigian 1990) for this reaction. Energetically, the spin-orbit constants for OH and NO are approximately the same and much smaller than the reaction exoergicity. An intriguing mechanism was proposed by Sauder and Dagdigian (1990) to rationalize this result. It was necessary to invoke the singlet-triplet couplings and electronic wavefunction symmetry considerations (both spatial and spin parts) similar to that for the infrared multiphoton dissociation  $HN_3$  case (Alexander *et al.* 1988b). They showed that the proposed mechanism could lead to an unequal spin-orbit population of the product if the product did not rotate too rapidly so that the preferred spin orientation along the quantization axis in the HONO\* complex could be transferred to the molecular axis in the free diatom. The different observations for the OH and NO spin-orbit populations depend on the fact that they are close to the Hund's case (b) and (a) descriptions respectively. In the former case, the spin is only weakly coupled to the diatomic axis. Thus the spin-orbit preference in the molecular frame is more likely to be washed out by rotation. Certainly this is an appealing mechanism, though it is unable to predict which spin state would be preferred. However, it is not clear how to reconcile this mechanism, which involves non-adiabatic couplings between the singlet-triplet surfaces, with that for  $\Lambda$ -doublet preference, which is essentially an adiabatic model. In particular, for a  $^2\Pi$  molecule the  $\Lambda$ -doublet states and spin-orbit manifolds are intrinsically non-separable. Recalling that in the Alexander treatment of the inelastic scattering of a  $^2\Pi$  radical with a closed-shell collision partner, both fine-structure effects are formulated in a coherent manner, section 3.1.2.

Secondly, there are a number of elegant u.v. photodissociation studies of the HONO molecule, both in the *trans*- (Vasudev *et al.* 1984, Shan *et al.* 1989a, Dixon and Rieley 1989) and *cis*- (Shan *et al.* 1989b) forms. The molecule absorbs in the near u.v. through a  $\pi^* \leftarrow n$ ,  $\tilde{A}^1A'' \leftarrow \tilde{X}^1A'$  transition centred on the  $-N=0$  chromophore. The absorption spectrum is structured with a long progression in the  $-N=0$  stretching mode, but the excited molecule predissociates and no rotational structure is discernible. Thus, it is a predissociative process with the vibrational state selectivity in the

electronically excited state. Asymptotically, this process leads to the same products as those from  $\text{H} + \text{NO}_2$ , that is  $\text{OH}(^2\Pi)$  and  $\text{NO}(^2\Pi)$ . Thus, the same PESs govern the exit channel at long range for both processes. It is interesting to note that the OH product from the photodissociation process exhibited a preferential production of  $\Pi(A')$   $\Lambda$ -doublet states (Vasudev *et al.* 1984), the same preference as that for  $\text{H} + \text{NO}_2$  but with a somewhat higher degree. On the other hand, unlike the statistical spin-orbit population in the OH product from  $\text{H} + \text{NO}_2$ , it was found that  $F_2(\Omega = \frac{1}{2}) > F_1(\Omega = \frac{3}{2})$  and this trend increased slightly with increasing photolysis wavelength. As for the NO photofragment, Dixon and Rieley (1989) found that  $\Pi(A'')$   $\Lambda$ -doublet states were preferentially populated. This, in conjunction with the finding for the OH fragment, seems to support the electronic wavefunction symmetry argument, as outlined in section 4.1. However, as pointed out by Dixon and Rieley, asymptotically the electronically excited  $\text{HONO}(\tilde{A}^1A'')$  can correlate adiabatically to either  $\text{OH}(^2\Pi(A')) + \text{NO}(^2\Pi(A''))$  or  $\text{OH}(^2\Pi(A'')) + \text{NO}(^2\Pi(A'))$ . Configuration mixing at short range between these two adiabatic channels is proposed as the main cause of the low degree of  $\Lambda$ -doublet specificity. A small degree of spin alignment in favour of the  $F_2(\Omega = \frac{3}{2})$  manifold of the NO product was also found, which is opposite to the reactive  $\text{H} + \text{NO}_2$  case. Spin-orbit mixing between the initially excited  $\text{HONO}(\tilde{A}^1A'')$  state and states of  $^3A'$  symmetry at long range was suggested to be the origin for this observation (Vasudev *et al.* 1984, Dixon and Rieley 1989). Hence, to interpret the spin-state distribution from either the photodissociation or chemical reaction, a similar spin-orbit coupling mechanism of inelastic scattering between the receding fragments was proposed, yet the spin selectivity in both OH and NO products from the two processes exhibit completely different behaviour. Unfortunately, the experiment on the inelastic scattering between OH and NO radicals has yet to be performed and the theoretical formalism needs to be developed to treat the inelastic scattering between two  $^2\Pi$  radicals. Nevertheless, this system provides a clear illustration of the intimate connections among the three processes; chemical reaction, photodissociation, and inelastic scattering in interpreting the observed fine-structure effects.

#### 4.2.2. $\text{CH} + \text{D}_2 \rightarrow \text{CD} + \text{HD}$

This is an isotope exchange reaction and hence is nearly thermoneutral. Only two PESs are involved, classified as  $^2A'$  and  $^2A''$  symmetry in planar geometry. The  $^2A'$  PES is mainly repulsive over the energy range of interest, while the  $^2A''$  PES leads to a deep well corresponding to the reactive intermediate, the  $\text{CHD}_2(\tilde{X}^2A'')$ . The reaction was thought to proceed by the addition-elimination mechanism on the  $^2A''$  surface. In fact, most of the thermal kinetic data has been satisfactorily interpreted in terms of a loose transition state statistical model (Berman and Lin 1984). At long range, both the entrance and exit channels are governed by the same  $^2A''$  and  $^2A'$  PESs as for the case of inelastic collision, section 3.2.1. Thus, conceptually, this is perhaps one of the simplest cases to explore the effects of multiple PESs on radical reaction and the intimate relationship between reactive and inelastic encounters.

In a recent study of this reaction, the state-to-state dynamics was characterized by the LIF technique under the single collision condition using a crossed-beam apparatus (Liu and Macdonald 1988, Macdonald and Liu 1989). At the rotational level of detail, the CD product distributions are shown in figure 7 for several collisional energies. Several features are worth commenting on. First of all, for most rotational levels there is a dramatic decrease in cross-sections with increasing collisional energy. Roughly speaking, this behaviour is in accord with the general expectation for a reaction



involving an intermediate complex, because of the decreasing probability for complex formation with increasing translational energy. Secondly, the energetic limits indicated by  $N_{\max}$  were not reached at higher collisional energies. In fact, compared to the simple PST calculations all observed distributions were considerably colder than the statistical predictions. Finally, note the appearance of the spikes at CH rotational levels  $N' = 3$  and 6. As can be seen from figure 7, these anomalous spikes are quite pronounced at  $E_0 = 1.5 \text{ kcal mol}^{-1}$  but become hardly detectable at  $E_0 = 4.5 \text{ kcal mol}^{-1}$ . This is a very dramatic dependence on the initial translational energy in view of a total energy greater than  $105 \text{ kcal mol}^{-1}$  is involved upon complex formation. Anomalies in the rotational level distribution for the inelastic scattering between  $\text{CH} + \text{D}_2$  were also

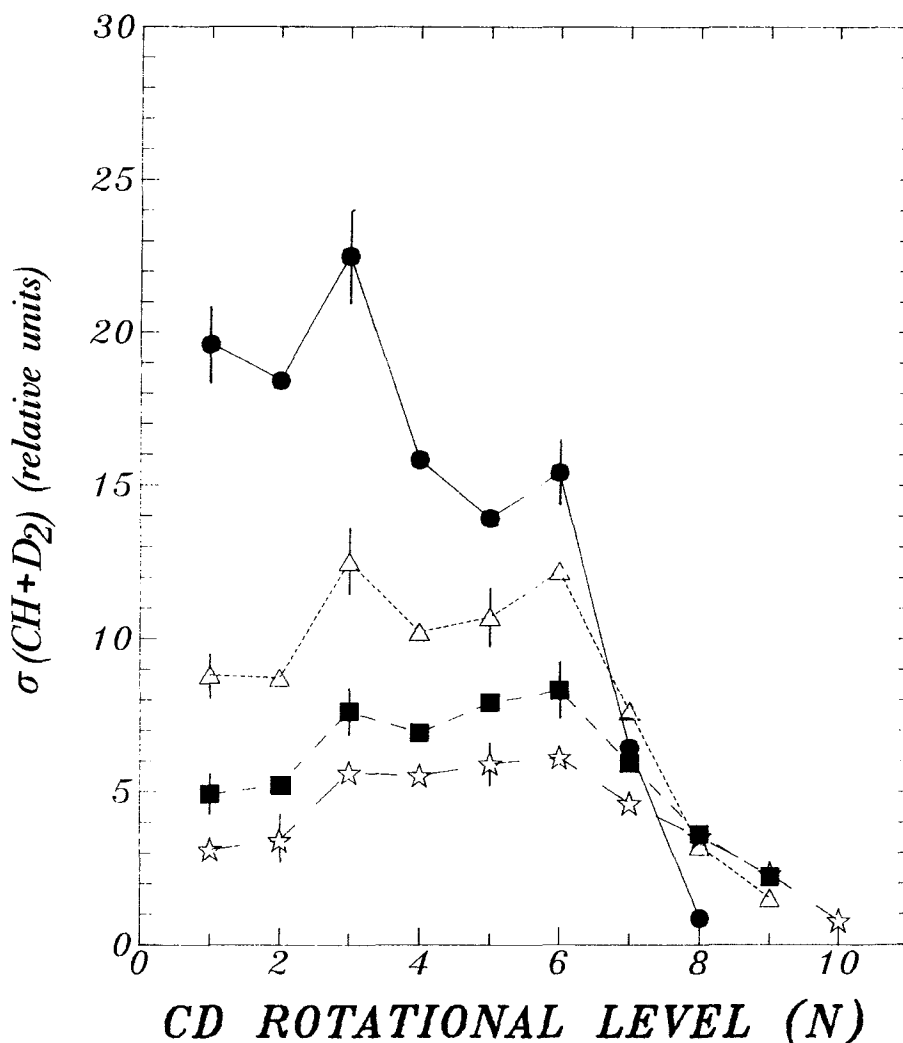


Figure 7. The rotational level distribution for reactive scattering of  $\text{CH}(N=1) + \text{D}_2 \rightarrow \text{CD}(N) + \text{HD}$  is shown at initial translational energies  $\bullet$  1.5,  $\triangle$  2.5,  $\blacksquare$  3.5 and  $\star$  4.5  $\text{kcal mol}^{-1}$ . The energetically accessible rotational levels,  $N_{\max}$ , are 8, 10, 12 and 14 respectively. From Macdonald and Liu (1990b).

observed and discussed in section 3.2.1. As mentioned there, these anomalies can be interpreted as arising from multiple-impact rainbow scattering. Because the PESs governing the entrance and exit channels are the same for the inelastic and isotope exchange processes, a similar mechanism of multiple-impact collisions between the dissociating CD and HD moieties could, conceivably, also manifest itself in the reactive scattering. Indeed, the proposed mechanism not only rationalized the observed product internal distribution being colder than that expected from a statistical decomposition, but also traced the occurrence of the spikes to a novel frequency-locking phenomenon between the two receding rotors, just as in the case of the inelastic scattering for  $\text{CH} + \text{D}_2$ . Similar anomalies were also observed in the reaction of  $\text{CD} + \text{H}_2 \rightarrow \text{CH} + \text{HD}$  (Macdonald and Liu 1990b). These observations, as well as the preliminary results of an extensive *ab initio* PES calculation (T. H. Dunning Jr and A. Wagner 1989, private communication), are all in support of the proposed mechanism.

As to fine-structure effects, figure 8 shows the results of the fine-structure state distribution for both CD and CH products from the reactions  $\text{CH} + \text{D}_2$  and  $\text{CD} + \text{H}_2$ , respectively. Clearly, the data indicate an erratic behaviour and a complete failure of the simple electronic symmetry argument. A closer examination of figure 8 reveals some order out of chaos. There is an out-of-phase oscillatory correlation between the fine-structure states with the same parity index e or f. This is in many aspects reminiscent of the situation reported in the state-to-state photodissociation studies (Hausler *et al.* 1987) of the first absorption band of  $\text{H}_2\text{O}$  molecule. Qualitatively many of the basic concepts involved for this reaction have already been described in section 4.1.2 for illustration. More specific and rigorous interpretations as to the exact origin of the behaviour seen in figure 8 has to await further theoretical developments. Nevertheless, a comparison of the fine-structure feature observed for the reactive channel with that for the inelastic one can be quite illuminating.

As discussed in section 3.1.2, the most striking fine-structure feature for a direct inelastic scattering involving a case (b) molecule in a  $^2\Pi$  state is the existence of orbital alignment resulting from quantum interference between the scattering amplitudes from the average and difference potentials. This propensity is generally expected to vary smoothly with respect to the rotational quantum number, as shown in figure 3 (a). By contrast, the fine-structure feature for a reactive scattering can be regarded as the net result of the effects in the transition state region and subsequent moderation by inelastic scattering. Two limiting cases arise. If the subsequent inelastic scattering dominates, then a similar behaviour to that for direct inelastic process might be anticipated. However, because the reaction paths for the two processes are not necessarily the same, the  $\Lambda$ -doublet component which will be preferred and the degree of preference could be different. For example, it is possible that  $V_{A''} > V_A$  globally, but  $V_{A''} < V_A$  locally. Nevertheless, theoretical treatments will be similar and the variation of the preference is expected to be relatively smooth for different rotational levels. On the other hand, if the effects in the transition state region dominate, then the fine-structure distributions can be erratic. The present case is an example, as shown in figure 8. The theoretical treatments will be system-dependent and, unlike the inelastic scattering, no general prediction can be made readily. Further differences between two limiting cases also prevail in the energy dependence. As shown in figure 3, the degree of orbital alignment from the inelastic channel is a strong function of initial translational energy, in particular near the threshold. By contrast, the fine-structure distribution for the isotope-exchange channel was found to be independent of the collisional energy (Macdonald and Liu 1990b). This situation is reminiscent of the wavelength

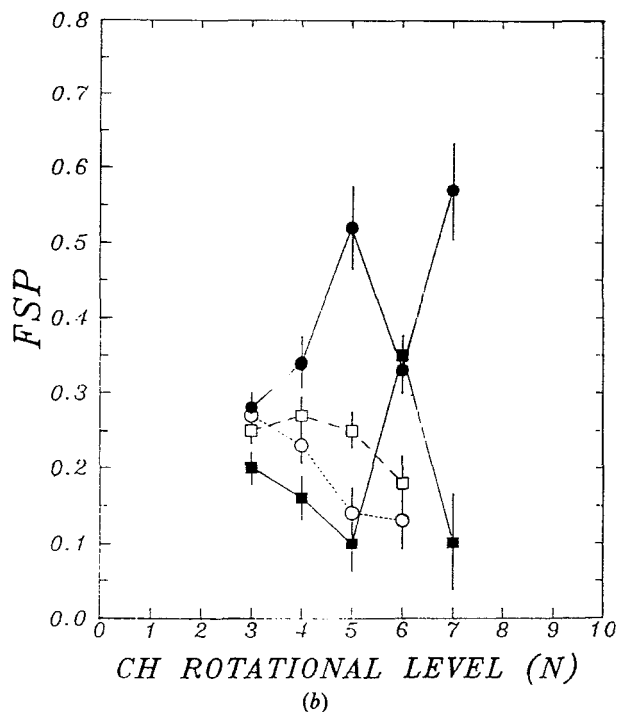
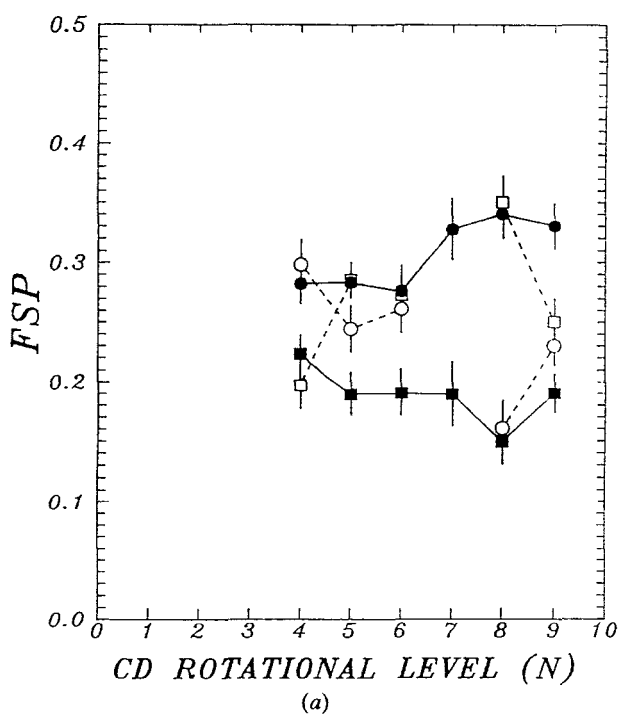


Figure 8. The fine-structure probability (FSP) is shown as distinct isotopic channels of the exchange reaction (a)  $\text{CH}(N=1) + \text{D}_2 \rightarrow \text{CD}(N') + \text{HD}$  and (b)  $\text{CD}(N=1) + \text{H}_2 \rightarrow \text{CH}(N') + \text{HD}$ . ● 1e, ○ 1f, □ 2f and ■ 2e. From Macdonald and Liu (1990b).

dependence in the direct photodissociation process (Andresen and Schinke 1988), in which the Franck–Condon model predicts little dependence on photolysis wavelength, while a strong dependence is expected if the final-state interactions dominate.

### 5. Perspectives

Gas phase chemical dynamics is a relatively mature field, yet there is much to be learned from state-to-state experiments, in particular for processes involving simple radicals. This article has tried to give a flavour of their breadth, value and current status. Clearly the surface is barely scratched, but what about the future?

On the inelastic side, as was seen from the discussions in section 3, the theoretical foundations laid down by Alexander and co-workers are now firmly established and confirmed experimentally (table 2) in the case of radical and spherically symmetric collision partners. To make a closer connection to the conceptual framework established for the closed-shell rotational energy transfer, as illustrated for the CH + He case, further theoretical work will be needed in order to relate the observed rainbow features to the anisotropies of the PESs. The theoretical treatment for the inelastic scattering process between two radicals is yet to be fully developed. Because this type of interaction often involves a chemical well, the treatment will be closely tied to that for a chemical reaction. As exemplified in the case of H + NO<sub>2</sub>, its precise description will provide invaluable insights into the origin of the fine-structure selectivity seen in many reactive and photodissociative events (table 3). Going beyond the diatomic radical, virtually nothing is known. For a diatomic radical it has been shown what kind of unique dynamic information is available from the  $\Lambda$ -doublet resolved measurements. For a closed-shell linear polyatomics there is analogous doubling of the rotational levels, the  $l$ -doubling which arises from the coupling between the rotational motion and the degenerate bending vibrations. The dynamical significance of  $l$ -doubling in an inelastic collision has been explored theoretically by Alexander and Clary (1983) and observed experimentally by Hershberger *et al.* (1988). A recent experiment on the rotational predissociation of the NeHF van der Waals molecule (Clary *et al.* 1988, O'Neil *et al.* 1989) is another excellent example of the dynamical consequence of  $l$ -doubling. However, for a linear polyatomic radical in a degenerate electronic state which is subject to the Renner–Teller effect, both  $\Lambda$ -type and  $l$ -type doublings contribute to the splitting (i.e. K-type doubling) in the energy levels. What can one learn about the collisional dynamics in such a system?

For a reactive or photodissociative process involving a radical with electronic orbital degeneracy, the situation is far from established. In fact, the state-to-state photodissociative experiments on the H<sub>2</sub>O molecule is the only case which has been satisfactorily explained in all respects. In this article, we outlined some intuitive, but perhaps somewhat provocative ideas about the fine-structure effects in these processes. We invite further theoretical work and experimental investigations in the future and hope that benefit will be gained from the intuitive ideas presented here.

As illustrated throughout this article, the product fine-structure selectivity, either in the spin-multiplet for a  $\Sigma$  radical or the  $\Lambda$ -doublet of a non- $\Sigma$  radical, in an inelastic collision often provides a sensitive, vectorial probe into the collisional dynamics. It is interesting to note that this is achieved without  $m_J$  being resolved. From a dynamical viewpoint, the fine-structure level of an open-shell species plays an analogous role as the magnetic sublevel of a closed-shell molecule. Similar results from a reactive or photodissociative process often carry a great deal of information about the interactions in the transition state or the Franck–Condon region, though a close collaboration with

theoretical investigations is essential before this information can be extracted. Like fine-structure splittings, hyperfine-structure splittings are manifestations of fundamental interactions within a molecule. Spectroscopically, the magnetic hyperfine interactions yield detailed information specific to the orbital and spin distributions of unpaired electrons, whereas the nuclear-electric quadrupole coupling describes electrostatic interactions involving all charged particles within the molecule. Though in an inelastic collision the nuclear spin can be approximated as a spectator, just like the electron spin, this may not be so in a process involving bond breaking and formation. We speculate that a systematic investigation of the hyperfine-structure effects in such cases may add a new dimensions to better our understanding of how a chemical reaction actually occurs.

### Acknowledgments

The significant contribution of Dr D. Sonnenfroh to the work in our laboratory is greatly appreciated. Stimulating discussions with Dr T. Dunning, Jr, Professors G. Schatz, P. J. Dagdigian and M. H. Alexander during the past several years are gratefully acknowledged. The authors thank Ms B. Rupp for her excellent preparation of this manuscript. K.L. would like to express his gratitude to Professors W. R. Gentry and C. F. Giese for teaching him everything about pulsed molecular beams. This work was supported by the U. S. Department of Energy, Office of Basic Energy Sciences, under contract no. W-31-109-ENG-38.

### References

- ALEXANDER, M. H., 1982, *J. chem. Phys.*, **76**, 5974; 1985, *Chem. Phys.*, **92**, 337.
- ALEXANDER, M. H., ANDRESEN, P., BACIS, R., BERSOHN, R., COMES, F. J., DAGDIGIAN, P. J., DIXON, R. N., FLYNN, G. W., GERICKE, E., GRANT, R., HOWARD, B. J., HUBER, J. R., KING, D. S., KINSEY, J. L., KLEINERMANN, K., KUCHITSU, K., LUNTZ, A. C., MCCAFFERY, A. J., POUILLY, B., REISLER, H., ROSENWAKS, S., ROTHE, E. W., SHAPIRO, M., SIMONS, J. P., VASUDEV, R., WIESENFELD, J. R., WITTIG, C., and ZARE, R. N., 1988a, *J. chem. Phys.*, **89**, 1749.
- ALEXANDER, M. H., and CLARY, D. C., 1983, *Chem. Phys. Lett.*, **98**, 319.
- ALEXANDER, M. H., and DAGDIGIAN, P. J., 1983, *J. chem. Phys.*, **79**, 302; 1984, *J. chem. Phys.*, **80**, 4325.
- ALEXANDER, M. H., DAVIS, S. L., and DAGDIGIAN, P. J., 1985, *J. chem. Phys.*, **83**, 556.
- ALEXANDER, M. H., and POUILLY, B., 1983, *J. chem. Phys.*, **79**, 1545.
- ALEXANDER, M. H., SMEDLEY, J. E., and COREY, G. C., 1986, *J. chem. Phys.*, **84**, 3049.
- ALEXANDER, M. H., WERNER, H.-J., and DAGDIGIAN, P. J., 1988b, *J. chem. Phys.*, **89**, 1388.
- ALI, A., and DAGDIGIAN, P. J., 1987, *J. chem. Phys.*, **87**, 6915.
- AL-IMARAH, F. J., BAIN, M. S., MEHDE, M. S., and MCCAFFERY, A. J., 1984, *J. chem. Phys.*, **82**, 1298.
- ALLIK, T. H., BRADY, B. B., FLYNN, G. W., and SPECTOR, G. B., 1984, *J. phys. Chem.*, **88**, 3204.
- ANDRESEN, P., 1986, *Comments atomic molec. Phys.*, **81**, 571.
- ANDRESEN, P., HAUSLER, D., and LULF, H. W., 1984, *J. chem. Phys.*, **81**, 571.
- ANDRESEN, P., and SCHINKE, R., 1988, *Molecular Photodissociation Dynamics*, edited by M. N. R. Ashford and J. E. Baggott (London: The Royal Society of Chemistry), p. 61.
- AOYAGI, M., SHEPARD, R., WAGNER, A. F., and DUNNING, JR, T. H., 1990, *J. phys. Chem.* (in the press).
- ARTHURS, M., and DALGARNO, A., 1960, *Proc. R. Soc. A*, **256**, 540.
- AUGUST, A., BROUARD, M., DOCKER, M. P., HODGSON, A., MILINE, C. J., and SIMONS, J. P., 1988, *Ber. Bunsenges phys. Chem.*, **92**, 264.
- BERGMANN, K., and DEMTRODER, W., 1971, *Z. Phys.*, **243**, 1; 1972, *J. Phys. B*, **5**, 1386.
- BERMAN, M. R., and LIN, M. C., 1984, *J. chem. Phys.*, **81**, 5743.
- BERNSTEIN, R. B., 1979, *Atom-Molecule Collision Theory. A Guide for the Experimentalist*, edited by R. B. Bernstein (New York: Plenum).
- BERNSTEIN, R. B., HERSCHBACH, D. R., and LEVINE, R. D., 1987, *J. phys. Chem.*, **91**, 5365.

- BERRY, M. T., BRUSTEIN, M. R., ADAMO, J. R., and LESTER, M. I., 1988, *J. phys. Chem.*, **92**, 5551.
- BIGIO, L., and GRANT, E. R., 1985, *J. phys. Chem.*, **89**, 5855.
- BONDYBEY, V. E., and ENGLISH, J. H., 1981, *J. chem. Phys.*, **74**, 6978.
- BRONIKOWSKI, M. J., ZHANG, R., RAKESTRAW, D. J., and ZARE, R. N., 1989, *Chem. Phys. Lett.*, **156**, 7.
- BROUARD, M., and O'MAHONY, J., 1988, *Chem. Phys. Lett.*, **149**, 45.
- BROWN, J. M., HOUGEN, J. T., HUBER, K. P., JOHNS, J. W. C., KOPP, I., LEFEBRE-BRION, M., MERER, A. J., RAMSAY, D. A., ROSTAS, J., and ZARE, R. N., 1975, *Molec. Spectrosc.*, **55**, 500.
- BROWN, L. C., WHITEHEAD, J. C., and GRICE, R., 1976, *Mol. Phys.*, **31**, 1069.
- BRUHLMANN, U., and HUBER, J. R., 1987, *Z. Phys. D.*, **7**, 1; 1988, *Chem. Phys. Lett.*, **143**, 199.
- BRUNNER, T. A., and PRITCHARD, D. E., 1982, *Adv. chem. Phys.*, **50**, 589.
- BUCK, U., 1986, *Comments atomic molec. Phys.*, **17**, 143.
- BUCK, U., OTTEN, D., SCHINKE, R., and POPPE, D., 1985, *J. chem. Phys.*, **82**, 202.
- BUTLER, J. E., JURSIK, G. M., WATSON, I. A., and WIESENFELD, J. R., 1986, *J. chem. Phys.*, **84**, 5365.
- CARRICK, P. G., and ENTGEKING, P. C., 1984, *Chem. Phys. Lett.*, **108**, 505.
- CAUGHEY, T. A., and CROSLY, D. R., 1979, *J. chem. Phys.*, **71**, 736.
- CHEN, P., COLSON, S. D., CHUPKA, W. A., and BERSON, J. A., 1986, *J. phys. Chem.*, **90**, 2319.
- CLARY, D. C., 1984, *Molec. Phys.*, **53**, 3; 1985, *Ibid.*, **54**, 605; 1987, *J. phys. Chem.*, **91**, 1718.
- CLARY, D. C., and HENSHAW, J. P., 1987, *Faraday Disc. chem. Soc.*, **84**, 333.
- CLARY, D. C., LOVEJOY, C. M., O'NEIL, S. V., and NESBITT, D. J., 1988, *Phys. Rev. Lett.*, **61**, 1576.
- CLOUTHIER, D. J., and KAROLCZAK, J., 1989, *J. phys. Chem.*, **93**, 7542.
- COREY, G. C., ALEXANDER, M. H., and DAGDIGIAN, P. J., 1986, *J. chem. Phys.*, **84**, 1547.
- COREY, G. C., and MCCOURT, F. R., 1983, *J. phys. Chem.*, **87**, 2723.
- CURL, R. E., MURRAY, K. K., PETRI, M., RICHNOW, M. L., and TITTEL, F. K., 1989, *Chem. Phys. Lett.*, **164**, 98.
- CURTISS, C. F., 1969, *J. chem. Phys.*, **79**, 1952.
- CURTISS, C. F., HIRSCHFELDER, J. P., and ADLER, F. T., 1950, *J. chem. Phys.*, **18**, 1638.
- DAGDIGIAN, P. J., 1988, *Atomic and Molecular Beam Methods*, edited by G. Scoles (Oxford University Press), Chaps. 23, 24; 1989a, *J. chem. Phys.*, **90**, 2617; 1989b, *Ibid.*, **90**, 6110.
- DAGDIGIAN, P. J., ALEXANDER, M. H., and LIU, K., 1989, *J. chem. Phys.*, **91**, 839.
- DAGDIGIAN, P. J., and BULLMAN, S. J., 1984, *J. chem. Phys.*, **81**, 3347; 1985, *Ibid.*, **82**, 1341.
- DAVIS, M., 1985, *J. chem. Phys.*, **83**, 1016.
- DEROUARD, J., 1984, *Chem. Phys.*, **84**, 181.
- DEWANGAN, D. P., FLOWER, D. R., and ALEXANDER, M. H., 1987, *Monat. Not. R. astron. Soc.*, **226**, 505.
- DEWANGAN, D. P., FLOWER, D. R., and DANBY, G., 1986, *J. Phys. B*, **19**, L747.
- DIETZ, T. G., DUNCAN, M. A., POWERS, D. E., and SMALLEY, R. E., 1981, *J. chem. Phys.*, **74**, 6511.
- DIXON, R. N., and RIELEY, H., 1989, *J. chem. Phys.*, **91**, 2308.
- DOCKER, M. P., HODGSON, A., and SIMONS, J. P., 1986, *Faraday Disc. chem. Soc.*, **82**, 25.
- DROEGE, A. T., and ENGELKING, P. C., 1983, *Chem. Phys. Lett.*, **96**, 316.
- DUFOUR, C., PINCHEMEL, B., DOUAY, M., SCHAMPS, J., and ALEXANDER, M. H., 1985, *Chem. Phys.*, **98**, 315.
- DUNLOP, J. R., KAROLCZAK, J., and CLOUTHIER, D. J., 1988, *Chem. Phys. Lett.*, **151**, 362.
- DUNNING JR, T. H., HARDING, L. B., BAIR, R. A., EADES, R. A., and SHEPARD, R. L., 1986, *J. phys. Chem.*, **90**, 344.
- FARTHING, J. W., FLETCHER, I. W., and WHITEHEAD, J. C., 1983, *J. phys. Chem.*, **87**, 1663.
- FAWZY, W. M., and HEAVEN, M. C., 1988, *J. chem. Phys.*, **89**, 7030.
- FOSTER, S. C., and MILLER, T. A., 1989, *J. phys. Chem.*, **93**, 5986.
- GENTRY, W. R., 1979, *Atom-Molecule Collision Theory. A Guide for the Experimentalist*, edited by R. B. Bernstein (New York: Plenum), Chap. 12.
- GENTRY, W. R., 1988, *Atomic and Molecular Beam Methods*, edited by G. Scoles (Oxford University Press), Chap. 3.
- GERICKE, K. W., KLEE, S., COMES, F. J., and DIXON, R. N., 1986, *J. chem. Phys.*, **85**, 4463.
- HABERLAND, P., ROHWER, P., and SCHMIDT, K., 1974, *Chem. Phys.*, **5**, 298.
- HABERLAND, P., VONLUCADOU, W., and ROHWER, P., 1980, *Ber. Bunsenges. phys. Chem.*, **84**, 507.
- HALL, G. H., LIU, K., MCAULIFFE, M. J., GIESE, C. F., and GENTRY, W. R., 1984, *J. chem. Phys.*, **81**, 5577.
- HAUSLER, D., ANDRESEN, P., and SCHINKE, R., 1987, *J. chem. Phys.*, **87**, 3949.
- HEAVEN, M., MILLER, T. A., and BONDYBEY, V. E., 1981, *Chem. Phys. Lett.*, **84**, 1; 1984, *J. chem. Phys.*, **80**, 51.

- HEFTER, U., and BERGMANN, K., 1988, *Atomic and Molecular Beam Methods*, edited by G. Scoles (Oxford University Press), Chap. 9.
- HERSCHBACH, D. R., 1987, *Chemica Scripta*, **27**, 327.
- HERSHBERGER, J. F., HEWITT, S. A., FLYNN, G. W., and WESTON, JR, R. E., 1988, *J. chem. Phys.*, **88**, 7243.
- HERZBERG, G., 1950, *Molecular Spectra and Molecular Structure I* (New York: Van Nostrand); 1966, *Molecular Spectra and Molecular Structure II* (New York: Van Nostrand).
- HOLLINGSWORTH, W. E., SUBBIAH, J., FLYNN, G. W., and WESTON JR, R. E., 1985, *J. chem. Phys.*, **82**, 2295.
- HUNTER, L. W., and CURTISS, C. F., 1973, *J. chem. Phys.*, **58**, 3884.
- HUNTER, L. W., and SNIDER, R. F., 1974, *J. chem. Phys.*, **61**, 5250.
- IP, P. C. F., BERNATH, R. F., and FIELD, R. W., 1981, *J. molec. Spectrosc.*, **89**, 53.
- IRVINE, A. M. L., SMITH, I. W. M., and TUCKET, R. P., 1989, *J. chem. Phys.* (submitted).
- JONES, P. L., GOTTFWALD, E., HEFTER, U., and BERGMANN, K., 1983, *J. chem. Phys.*, **78**, 3838.
- JOSWIG, H., ANDRESEN, P., and SCHINCKE, R., 1986a, *J. chem. Phys.*, **85**, 1904.
- JOSWIG, H., O'HALLORAN, M. A., ZARE, R. N., and CHILD, M. S., 1986b, *Faraday Discuss. chem. Soc.*, **82**, 79.
- KANAMORI, H., BUTLER, J. E., KAWAGUCHI, K., YAMADA, C., and HIROTA, E., 1985, *J. chem. Phys.*, **83**, 611.
- KLEINERMANN, K., LINNEBACH, E., and POHL, M., 1989, *J. chem. Phys.*, **91**, 2181.
- KLENERMAN, D., and SMITH, I. W. M., 1987, *J. chem. Soc. Faraday Trans. II*, **83**, 229.
- KOCHANSKI, E., and FLOWER, D. R., 1981, *Chem. Phys.*, **57**, 217.
- KOK, R., WAGNER, A., and DUNNING JR, T. H., 1990 (in preparation).
- KOURI, D. J., 1979, *Atom-Molecule Collision Theory. A Guide for the Experimentalist*, edited by R. B. Bernstein (New York: Plenum), Chap. 9.
- LAHMANI, F., LARDEUX, C., and SOLGADI, D., 1986, *Chem. Phys. Lett.*, **129**, 24.
- LEE, Y. T., 1987, *Science*, **236**, 793.
- LEMOINE, D., COREY, G. C., ALEXANDER, M. H., and DEROUARD, J., 1987, *Chem. Phys.*, **118**, 357.
- LENGEL, R. K., and CROSLLEY, D. R., 1977, *J. chem. Phys.*, **67**, 2085.
- LEVINE, R. D., and BERNSTEIN, R. B., 1987, *Molecular Reaction Dynamics and Chemical Reactivity* (Oxford University Press).
- LIGHT, J. C., 1967, *Faraday Discuss. chem. Soc.*, **44**, 14.
- LIGHT, J. C., and ALTENBERGER-SICZEK, A., 1976, *J. chem. Phys.*, **64**, 1907.
- LIU, K., and MACDONALD, R. G., 1988, *J. chem. Phys.*, **89**, 4443.
- MACDONALD, R. G., and LIU, K., 1989, *J. chem. Phys.*, **91**, 821; 1990a, *Ibid.* (submitted); 1990b, *Ibid.* (submitted).
- MARIELLA, R. P., LANTZSCH, B., MOXSON, V. T., and LUNTZ, A. C., 1978, *J. chem. Phys.*, **69**, 5411.
- MARIELLA, R. P., and LUNTZ, A. C., 1977, *J. chem. Phys.*, **67**, 5388.
- MATSUMI, Y., MUNAKATA, T., and KASUYA, T., 1984, *J. chem. Phys.*, **81**, 1108.
- MAYAMA, S., HIRAOKA, S., and OBI, K., 1984, *J. chem. Phys.*, **80**, 7.
- MCGUIRE, P., and KOURI, D. J., 1974, *J. chem. Phys.*, **60**, 2488.
- MILLER, T. A., 1982, *Ann. Rev. phys. Chem.*, **33**, 257; 1984, *Science*, **223**, 545.
- MONTS, D. L., DIETZ, T. G., DUNCAN, M. A., and SMALLEY, R. E., 1980, *Chem. Phys.*, **45**, 133.
- MURPHY, E. J., BROPHY, J. H., and KINSEY, J. L., 1981, *J. chem. Phys.*, **74**, 331.
- NAULIN, C., COSTES, M., and DORTHE, G., 1988, *Chem. Phys. Lett.*, **143**, 496.
- NEDELEC, O., and DUFAYARD, J., 1984, *Chem. Phys.*, **84**, 167; 1986, *Chem. Phys.*, **105**, 371.
- O'NEIL, S. V., NESBITT, D. J., ROSMUS, P., WERNER, H.-J., and CLARY, D. C., 1989, *J. chem. Phys.*, **91**, 711.
- OBI, K., MATSUMI, Y., TAKEDA, Y., MAYAMA, S., WATANABE, H., and TSUCHIYA, S., 1983, *Chem. Phys. Lett.*, **95**, 520.
- OGAI, A., QIAN, C. X. W., IWATA, L., and REISLER, H., 1988, *Chem. Phys. Lett.*, **146**, 367.
- OTTINGER, C., and POPPE, D., 1971, *Chem. Phys. Lett.*, **8**, 513.
- OTTINGER, C., VELASCO, R., and ZARE, R. N., 1970, *J. chem. Phys.*, **52**, 1636.
- PACK, R. T., 1974, *J. chem. Phys.*, **60**, 633.
- PAULY, H., and TOENNIES, J. P., 1965, *Adv. atomic mol. Phys.*, **1**, 195.
- PECHUKAS, P., LIGHT, J. C., and RANKIN, C., 1966, *J. chem. Phys.*, **44**, 794.
- POLANYI, J. C., 1972, *Acc. chem. Res.*, **5**, 161; 1987, *Chemica Scripta*, **27**, 229.
- QUACK, M., 1979, *J. phys. Chem.*, **83**, 150.
- QUACK, M., and TROE, J., 1974, *Ber. Bunsenges. phys. Chem.*, **78**, 240.

- QUINTON, A. M., and SIMONS, J. P., 1981, *Chem. Phys. Lett.*, **81**, 214.
- ROBINSON, G. N., NATHANSON, G. M., CONTINETTI, R. E., and LEE, Y. T., 1988, *J. chem. Phys.*, **89**, 1988.
- SAUDER, D. G., and DAGDGIAN, P. J., 1990, *J. chem. Phys.*, **92**, 2389.
- SAUDER, D. G., PATEL-MISRA, D., and DAGDIGIAN, P. J., 1990, *J. chem. Phys.*, **91**, 5316.
- SCHINKE, R., 1981a, *J. chem. Phys.*, **75**, 5205; 1981b, *Ibid.*, **75**, 5449; 1986, *J. phys. Chem.*, **90**, 1742.
- SCHINKE, R., and ANDRESEN, P., 1984, *J. chem. Phys.*, **81**, 5644.
- SCHINKE, R., and BOWMAN, J. M., 1983, *Molecular Collision Dynamics*, edited by J. M. Bowman (Heidelberg: Springer), Chap. 4.
- SCOLES, G., 1988, *Atomic and Molecular Beam Methods*, edited by G. Scoles (Oxford University Press).
- SECRET, D., 1979, *Atom-Molecule Collision Theory. A Guide for the Experimentalist*, edited by R. B. Bernstein (New York: Plenum), Chap. 8.
- SHAN, J. H., VORSA, V., WATEGAONKAR, S. J., and VASUDEV, R., 1989a, *J. chem. Phys.*, **90**, 5493.
- SHAN, J. H., WATEGAONKAR, S. J., and VASUDEV, R., 1989b, *Chem. Phys. Lett.*, **160**, 614.
- SILVER, J. A., DIMPTL, W. L., BROPHY, J. H., and KINSEY, J. L., 1976, *J. chem. Phys.*, **65**, 1811.
- SMITH, I. W. M., 1980, *Kinetics and Dynamics of Elementary Gas Reactions* (London: Butterworths).
- SONNENFROH, D., MACDONALD, R. G., and LIU, K., 1990 (in preparation).
- SPENCER, J. E., and GLASS, G. P., 1976, *Chem. Phys.*, **15**, 35.
- STEPHENSON, J. C., CARASSA, M. P., and KING, D. S., 1988, *J. chem. Phys.*, **89**, 608.
- STEPSOWSKI, D., and COTTEREAU, M. J., 1981, *J. chem. Phys.*, **74**, 6674.
- TICKTIN, A., BRUNO, A. E., BRUHLMANN, U., and HUBER, J. R., 1988, *Chem. Phys.*, **125**, 403.
- TRUHLAR, D. G., HASE, W. L., and HYNES, J. T., 1983, *J. phys. Chem.*, **87**, 2264.
- VAN DE BURGT, L. J., and HEAVEN, M., 1987, *J. chem. Phys.*, **87**, 4235.
- VASUDEV, R., ZARE, R. N., and DIXON, R. N., 1984, *J. chem. Phys.*, **80**, 4863.
- WAGNER, A., and ALEXANDER, M. H., 1990 (in preparation).
- WAGNER, A. F., and PARKS, E. K., 1976, *J. chem. Phys.*, **65**, 4343.
- WICKRAMARATCHI, M. A., SETSER, D. W., HILDEBRANDT, B., KORBITZER, B., and HEYDTMANN, H., 1984, *Chem. Phys.*, **84**, 105.
- WITTIG, C., NADKI, I., REISLER, H., NOBLE, M., CATANZANTE, J., and RADHAKRISHNAN, G., 1985, *J. chem. Phys.*, **83**, 5581.
- YARKONY, D. R., 1989a, *J. chem. Phys.*, **89**, 4945; 1989b, *Ibid.*, **90**, 1657.